

Impact of the urban design on Urban Heat Islands: The Use and Possibilities of Thermal Satellite Imagery



Jurek van Goor
6591221
j.vangoor@students.uu.nl

Dr. A. Rafiee
Prof. dr. ir. Peter van Oosterom

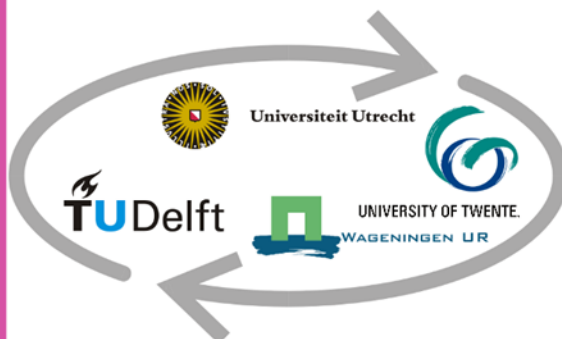


Table of contents	Page
Summary	3
1. Introduction	4
2. Literature review	6
2.1 Urban Heat Island	6
2.3 Thermal Sensors	7
2.3 Urban Design	7
3. Methodology	10
3.1 Data	10
3.1.1 Land Surface Temperature	10
3.1.2 Air temperature	11
3.1.3 The BAG	11
3.1.4 Street Network	11
3.1.5 Water	11
3.1.6 Vegetation	11
3.1.7 Slope	12
3.1.8 Sky View Factor	12
3.1.9 Low albedo surfaces	12
3.2 Analysis	12
3.2.1 Research area	12
3.2.2 Data	13
3.2.3 Land Surface Temperature	14
3.2.4 Building age	15
3.2.5 Building height	16
3.2.6 Entropy	16
3.2.7 Water surface	16
3.2.8 Green	17
3.2.9 Slope	17
3.2.10 Sky View Factor	17
3.2.11 Multi linear regression	19
3.2.12 Spatial Autocorrelation	19
3.2.13 Geographically weighted regression	20
3.3 Software	20
3.4 Scope	21
4. Results	22
4.1 Spatial autocorrelation	22
4.2 Geographically weighted regression	27
4.3 Multiple linear regression	29
5. Conclusion	33
6. Discussion	35
6.1 Entropy values	35
6.2 Sky view factor	35
6.3 Slope and Aspect	35
6.4 Results	35
6.5 Recommendations	36
7. Literature	37
8. Appendix	41

Summary

This thesis is about the use of thermal imagery sensors mounted to satellites to retrieve Land Surface Temperature data in the research to Urban Heat Islands. The purpose of the thesis is to see whether the UHI data derived from the LST will be similar to current and accepted models of UHI's based on the air temperature. Furthermore different urban design features such as, the percentage of green, the height of the green, the amount of water surface, the surface area of low albedo surfaces, the building age, the Sky View Factor, entropy and slope will be researched if they have a significant impact on the Urban Heat Island effect based on Land Surface Temperature. For this research several methods are used. To see whether the UHI data derived from the LST corresponds with the UHI data from the models a spatial autocorrelation is done to see whether the LST data is clustered together. Also a geographically weighted regression is done. The results of the geographically weighted regression show if the UHI effect based on the LST explain and correspond with the differences in the UHI effect based on the air temperature. In addition a multiple linear regression is carried out to get an insight on which of the urban design features have an effect on the UHI effect based on the LST. The most important results are that the UHI effect based on LST on both the neighbourhood and the sub neighbourhood level show a clustered pattern which is expected from temperature data. Also the UHI effect based on LST has a very strong correlation with the UHI effect based on air temperature. The urban features that significantly correlated with the UHI effect based on LST are the percentage of green, the amount of water surface, the surface area of low albedo surfaces and the building age. From these the low albedo surface area has a positive correlation and the other features have a negative correlation. Recommended for future studies is to expand the research area and also include dates which are less warm and sunny to compare the UHI effect based on LST with the UHI effect based on air temperature.

1. Introduction

The concept of the urban heat island first came to research in the a book of Luke Howard in 1818. However in this book the term urban heat island is not mentioned. He research the climate in the United Kingdom and London (Howard, 2012). Later on from 1920 to 1940 different researchers in the field of local climatology tried to get more understanding in the phenomenon. In 1929 it is believed that the term urban heat island is first used by Albert Pepler (Stewart, 2019). From the 1990's onwards the subject of urban heat islands began to increase in popularity with most articles being published from 2015 onwards (Masson et al, 2020). This might be due to occurring climate change which becomes more and more to our knowledge the last few years. The increase in temperature might also increase the severity of Urban heat Islands.

National Geographic gives the definition of an urban heat island as "a metropolitan area that is a lot warmer than the rural areas surrounding it" (National Geographic, n.d.). Urban heat islands especially occur in places with lots of activity and lots of people. This is because heat is created by energy from all the cars, busses, trains and activity from the people in the city. Especially in big cities for example Paris or New York the urban heat islands occur (National Geographic, n.d.). Urban heat islands can cause problems in the cities where they occur. The urban heat islands contribute to higher temperatures during the day time, reduced cooling during the night time and a higher level of air pollution (United States Environmental Protection Agency, 2022). These factors in turn can be related and contribute to heat related deaths and heat related illnesses such as non-fatal heat strokes, heat cramps, heat exhaustion, respiratory difficulties, or general discomfort (United States Environmental Protection Agency, 2022). The Urban Heat Islands can also amplify the effects of naturally occurring heat waves. These are periods of weather conditions being hotter and more humid than normal. The sensitive population groups are especially at risk during these events (United States Environmental Protection Agency, 2022). These sensitive populations consist of; older adults, young children, people with low income, people who work outdoors, and people in poor health. From 2004 to 2018 a total of 10.527 of heat related deaths were reported in the United States. This is an average of 702 deaths per year due to the heat. The numbers include deaths as well as where heat was the contributing cause as deaths where heat was the underlying cause (Vaidyanathan et al, 2020).

These numbers show the severity of the problem because not only in the United States the temperatures in cities can cause fatal and non-fatal issues to people, this can happen all across the world as studies have shown (Wong, Paddon & Jimenez, 2013). They state in their article many cities across the world where urban heat islands occur. Some examples are Buenos Aires in Argentina, Wroclaw in Poland, Rotterdam in the Netherlands, Taipei in Taiwan, Washington DC in the USA, and Akure in Nigeria. This list contains many more cities and comes from an article in 2013 which gives the possibility that in the meantime the situation has developed (Wong, Paddon & Jimenez, 2013). In the article they mention Hong Kong, Bangkok, Delhi, Bangladesh, London, Kyoto, Osaka, and Berlin as cities where increased mortality rates can be linked to heightened temperatures during non-heatwave periods (Wong, Paddon & Jimenez, 2013). Later on more studies have been done regarding urban heat islands and to a lesser extent also the fatalities. The latter mainly focussing on the USA and some individual cities in other locations on the world (Paravantis et al, 2017; Ramamurthy & Bou-Zeid, 2017). Furthermore research has been conducted multiple times on the causes, effects and how to mitigate the effect of urban heat islands (Nuruzzaman, 2015; Mohajerani, Bakaric & Jeffrey-Bailey, 2017; Vujovic et al, 2021). Most of the scientific papers focus on the type of surface area like asphalt or the reflectance of the pavement. But research is also done for other urban features like building types, building configuration, vegetation and road configuration. These are factors that might also influence urban heat islands. What can also develop the efficiency and way of research to urban heat islands is the enhancement of advanced technologies in this field of research. With advanced technologies in

this case is meant the use of satellite imagery, efficient spatial data management and usage, and the usage of further developed software regarding the collection of data but also the further editing and analysis of the data. When searching through scientific articles satellite imagery can be used for observing the growth of crops, the detection of objects or change detection in for example land use. However the opportunities in the research of Urban Heat Islands are also possibilities of satellite imagery. The instruments mounted to the satellites have improved over the last years (Zhao-Liang, Sobrino and Song, n.d.). This makes it worthy to also take a look at how Land Surface Temperature data from satellites can be useful in the research of UHI's. As stated by the book of Khan, Chatterjee and Wang (2020) Land Surface temperature or LST is radiative temperature of the land derived from solar temperature. LST measures the emission of thermal radiance from the land surface where the incoming solar energy interacts with and heats the ground or the surface of canopy in vegetated areas. The LST value is a mixture between bare soil temperatures and the temperature of vegetation. Most of the studies on UHI's focus on the summer periods. In this research the summer will also have the focus. This is because the temperatures in the summer are highest and then have the biggest impact on factors like increased energy consumption, an elevation of air pollutants and greenhouse gases, a compromise of human health and comfort, and impaired water quality (EPA, n.d.). Furthermore focus will be on the usability of satellite imagery for the analysis of urban heat islands on a larger scale in different neighbourhoods of the urban environment. This is because the combination of using LST data and different features of the urban structure possibly generate new knowledge in the already existing literature. The choice for different neighbourhoods will help by generating results which building types and configuration, vegetation or road configuration influences the urban heat islands based on LST and what does not. For this research data from a thermal sensor which is mounted to a satellite will be used to gather the temperature values of the corresponding neighbourhoods. However before this can be done further information needs to be gathered on how data from a thermal sensor can be used to measure surface temperatures. Therefore for this research the following research question is formulated.

- What urban design features in different neighbourhoods of cities in the Netherlands have an influence on urban heat islands over time?

With the following sub questions

- How can data from a thermal sensor mounted to a satellite be used to measure the temperature of a neighbourhood?
- What is the use of thermal imagery to estimate the Urban Heat Island effect?
- Which indicators can be defined as the proxy for a neighbourhoods spatial configuration?

The Different characteristics of neighbourhoods that will be researched will further be explained during the method however some hypothesis can already be formulated.

Hypothesis 1: Expected is that Land Surface Temperature based on satellite imagery can be a useful data in mapping the Urban Heat Island effect at different circumstances.

Hypothesis 2: Expected is that the age of buildings because of generally worse insulation, taller buildings close to each other, a grid like street pattern, and non-reflective surfaces such as asphalt or concrete will increase the phenomenon of urban heat islands.

Hypothesis 3: Expected is that a higher percentage of urban green, a more organic street pattern, modern housing and waterways will decrease the phenomenon of urban heat islands.

During this research the hypothesis will be tested and an answer will be formulated. The results will contribute to a better understanding of the topic and can lead to better policies solving and preventing the problem on a local level. Also it can generate a new insight into methodologies for the research on UHI's.

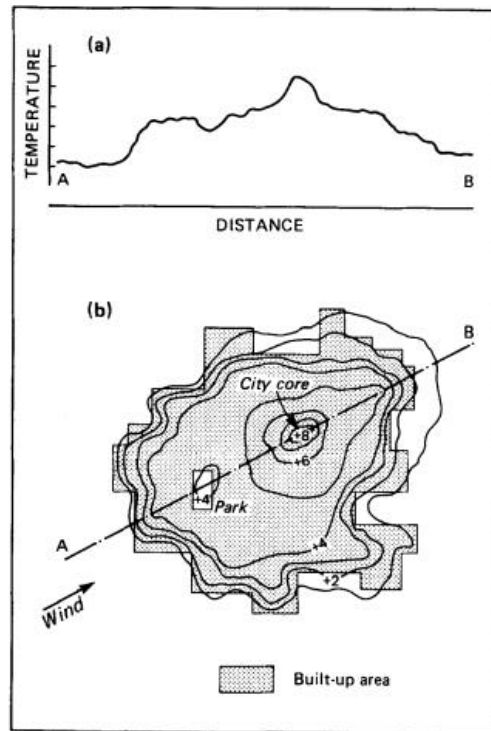
2. Literature review

2.1 Urban heat Island

To research the topic the concept of Urban Heat Islands needs to be understood first. The Urban Heat Island effect is when the development of temperature in the city is noticeably higher compared with the countryside that directly neighbours the same city (Santamouris, 2015). The concept of urban heat islands has already been well researched. The research from Oke (1982) mentions research that has already been done on the topic of the Urban Heat Island effect and comes to a conclusion that the Urban Heat Island effect shows the same in towns, villages and cities. In the same paper Oke (1982) mentioned that the temperature increase in the city compared to the rural area can be between 2 and 8 degrees Celsius higher due to the Urban Heat Island effect with the highest temperatures being located in the city centre. However more recent studies show a higher difference in temperature between the rural area and the city (WUR, n.d.; Santamouris, 2013). Several causes have been given to the effect of urban heat islands. The changing nature of the cities we live in like the reduction in vegetation and evaporation, a higher amount of dark surfaces with low reflection, and more emission of heat by for example cars or air conditioning are all given causes (Stone, Hess and Frumkin, 2010). Studies in the USA have shown that an average city there is characterised by 29-39 percent of paved surface, 19-25 percent roofs, and 29-41 percent vegetation. This indicates that in an American city over 60 percent of an urban surface is manmade which often is heat absorbent (Arbari & Rose, 2008). Arbari and Rose (2008) have concluded in their paper that knowledge of the surface conditions and urban environment is important to come to measures for the mitigation of the urban heat island effect.

As mentioned before in the article from Oke in 1982 it was already illustrated that the highest temperature in the city is located in its centre. The temperature gradually rises from the edges of the city into the centre where the temperature spikes. With new innovations in the building environment this pattern is tried to be mitigated. An example of this is using high solar reflective materials for new buildings. This can decrease the surface temperatures which in turn lower the air temperature but the reflected solar radiation can increase the temperature of the surrounding built up environment and therefore increase their cooling load (Yang, Wang & Kaloush, 2015). Another research of Mohajerani, Bakaric and Jeffrey-Bailey (2017) mainly focusses on the different surfaces in the city such as the pavement or asphalt and what to do to mitigate the effect of temperature of these materials. These studies on different materials on buildings and the surface show that the research on how to mitigate the effect of urban heat islands continues further. However when looking further into outlines of the Urban Heat Island in the earlier research of Oke (1982) the curve on how the urban environment heats up as seen in figure 1 with the highest temperature in the centre and lower temperatures the further you travel from the centre might give some new insights in the mitigation of urban heat islands. If by different measures the temperature is lowered the urban environment around the city centre this lower surrounding temperature might also influence the temperature in the city centre. However before this can be researched more knowledge needs to be gathered about how neighbourhoods in the urban area contribute to the Urban Heat Island effect and which characteristics of neighbourhoods have an influence on the Urban Heat Island effect.

Figure 1, The spread of urban heat island through a city



Oke, T. R. (1982). The energetic basis of the urban heat island. *Quarterly Journal of the Royal Meteorological Society*, 108(455), 1-24.

2.2 Thermal sensors

All objects that have a temperature higher than absolute zero which is 0 Kelvin or -273.15 degrees Celsius emit radiation (Li et al, 2013). This radiation can be detected by a thermal sensor. That thermal sensor measures the amount of infrared radiation coming from the object or in this case the surface of the earth. The sensor is a Thermal Infrared Sensor. This type of sensor applies quantum physics to detect heat (NASA, 2013). A thermal infrared sensor mounted to a satellite uses Quantum Well Infrared Photodetectors which detect long wavelengths of light emitted from the earth of which the intensity depends on the surface temperature (NASA, 2013). Thermal imaging applications in Earth observation are for example the monitoring of wildfire, droughts, the weather or urban heat islands (Rieke, 2021). There are multiple satellites which carry sensor with thermal bands. Some examples are Landsat 8, Sentinel-3, MODIS or AVHRR. But for none of those the main focus lays on thermal imaging (Rieke, 2021). Often the spatial resolution is quite low in the range of 100 meter which is the case for Landsat 8. Thermal sensors mounted to an airplane or UAV can reach higher resolutions of a few meters however these methods of gaining data are much more expensive and not scalable for the monitoring of many varied locations (Rieke, 2021).

2.3 Urban Design

When looking into the different indicators and their effect on urban heat islands some research has already been done mainly on a city scale. The age of the buildings could mainly influence the urban heat island effect if it turns out that older buildings lose more heat than newer ones (Vujovic et al, 2021). This can be due to poorer insulation used when those buildings are built compared to newer techniques. Studies have shown this result, the older the housing the higher the average air leakage is

from inside the house to the outside or the other way around (Khemet & Richman, 2018). Also the height of buildings can influence the urban heat. Research conducted taking into account the height of buildings shows differing results. A study more focused on the flow of air around tall buildings indicate that tall buildings help increase flow of air into certain streets however by removing them a reduced height in buildings helps to ventilate the space uniformly which creates a more naturally ventilated area (Rajagopalan, Lim & Jamei, 2014). The research of Nichol (2005) on the other hand states that the hottest areas are where no tall buildings are located. The hotter areas mainly focus around low rise residential developments, open spaces such as car parks or a bus depot. Low rise residential buildings are buildings three stories or less in height (FEMA, 2020).

In addition research will be conducted if urban heat islands can also be linked to the configuration of street networks in neighbourhoods. Mainly the focussing on the street networks with its density and morphology. There are four main urban morphological types. These are a grid system, a radial form, a linear form and an irregular or organic form (Agirbas & Ardaman, 2017; Lynch & Hack, 1984). A grid is clear and easy to follow for traffic. An example of a grid city is Chicago, in this city the streets are connected square with each other (Boeing, 2019). The radial form is another type of urban morphology. The street network expands its spread out from the centre of the city. An example of a radial city is Rome (Lynch & Hack, 1987). The third general pattern is the linear system. It consists of a single line to which all destinations and origins are attached. The linear system is mainly used along freight railways, canals and highways. An example of a linear city is Brighton (Margaritis & Kang, 2016; Lynch & Hack, 1984). An irregular morphology is a more random city pattern. The form of the city is organic. It is the opposite of a planned city. This form does not comply with the grid, radial or linear patterns. An example can be the city of Soa Paolo (Agirbas & Ardaman, 2017). Although there is not much research done regarding the street patterns and urban design in regard to Urban Heat Islands. However it has to be set that some is done. The research from Stone Jr and Rodgers (2001) indicates that a higher density of street intersections has a lower heat production. This could mean that a grid like street pattern could positively mitigate the effect of urban heat islands, although this must be researched before making a statement. In this research the urban morphology is defined by entropy as Boeing (2019) describes in the article. The entropy of a city's street network is a measure for the degree of its order. Cities with a grid pattern and ordered street will have a low entropy value. Cities with an organic street pattern have a higher entropy, which means they are more disordered (Boeing, 2019).

The effect of water and urban green on urban heat islands have been researched before. A research in Athens from Zoulia, Santamouris and Dimoudi (2009) showed that on the city scale the area with urban green, which was the neighbourhood of a city park in their research had a lower temperature. The difference in temperature between the green area within the city and surrounding neighbourhoods was especially greater during the night. But during the day the difference was still significant. The research showed that having a park in the city does not significantly influence the Urban Heat Island effect of the surrounding neighbourhoods but characteristics in the neighbourhoods themselves have the greater influence (Zoulia, Santamouris & Dimoudi, 2009). This gives an indication green has to be implemented in the neighbourhoods themselves instead of in parks around the city. Furthermore the research from Steeneveld, Koopmans and Heusinkveld (2014) state that urban water bodies influence the urban microclimate. In their research the harbour area surrounded by water has a lower temperature during the day time whilst during the night-time the temperature is very similar to the temperature in the city centre. More research on the effect of water on urban heat islands can be useful especially on a smaller scale or smaller bodies of water.

At last the effect of different kinds of surfaces and their ability to reflect sunlight. The paper of Nuruzzaman (2015) gives low albedo materials as one of the primary causes of urban heat island. The albedo is given by the ratio of the reflected solar energy to the incident solar energy. The albedo of a

city can differ greatly due to different factors such as the orientation, heterogeneity and materials used in the environment (Nuruzzaman, 2015). If the albedo is low less energy will be reflected and more energy will be stored in the surface which will increase the urban temperature and the other way around. The analysis of this research will focus on materials with a low albedo as input data.

Due to the ongoing climate change the situation regarding Urban Heat Island keeps changing which makes continuation of research in the possible solutions and measurements necessary.

3. Methodology

For this research the following methodology is used. To get more insight in the usability of thermal imagery in the research to Urban Heat Islands a spatial autocorrelation and geographically weighted regression are done. With these test it will be checked if the UHI based on Land Surface Temperature has the same characteristics as the UHI based on air temperature. Also a multiple linear regression is done to check whether or not there is a relationship between different urban characteristics and the UHI effect based on LST. A flow chart of the methodology with all the input data is given in appendix 1.

3.1 Data

3.1.1 Land Surface Temperature

The data that will be used will be from different sources. The most important data on the temperature in different neighbourhoods in the city will be derived from the ECOSTRESS instrument this is an abbreviation for ECOSystem Spaceborne thermal Radiometer Experiment on Space Station. This is an existing thermal infrared radiometer put on the International Space Station. It gives the land surface temperature in a 70 meter resolution (Cawse-Nicholson, 2019). Data from this instrument is available for at least once every day during the day time but most often multiple times per day from January 2019 to February of 2023. This is a total of 1.1 TB of data. However for the research itself only certain time periods need to be researched and not all data will be useful due to clouds blocking the instrument. The ECOSTRESS land surface temperature product uses a physics based algorithm Temperature Emissivity Separation to retrieve the Land Surface Temperature from five different ECOSTRESS thermal infrared bands with wavelengths between 8 and 12.5 μm (Chang et al, 2021). Different research has shown that the instrument has an accuracy at the level of 1 Kelvin over all land surface types (Chang et al, 2021). In addition the Land Surface Temperature product is validated by the ECOSTRESS science team (Hook et al, 2020). That science team reported a uncertainty of the product below 1 K. More recent validation efforts on the instrument showed that the mean absolute error is 0.4 K with an $R^2 > 0.988$ on average for all global validation sites used for the research (Hulley et al, 2021). Downloading information from the ECOSTRESS instrument is done through the AppEEARS application from NASA and USGS which are the National Aeronautics and Space Administration and the United States Geological Survey. Both organisations are involved in research from satellites (U.S. Geological Survey, n.d.; NASA, 2023). When downloading from the AppEEARS site you can choose the location of your research for which the data will be retrieved. The data does not always perfectly align the area selected. This is because these are static images from a satellite taken at an angle in comparison to the earth's surface. If the image only contains part of the research area the application gives you the option to download more images which later can be laid next to each other and be combined in software like ArcGIS pro to cover the entire research area. These images are from the same time so it will not create inconsistencies within the data. Because data of the ECOSTRESS LST product is already given in temperature Kelvin instead of the amount of radiation there is no need to give an explanation on how certain levels of radiation can be recalculated in exact temperatures for this research. For an Urban Heat Island analysis it is preferable to have the air temperature instead of the land surface temperature. However calculating the air temperature with the available resources of this research will not be feasible. Research from Tomlinson et al (2011) states that; *"LST and air temperature are not directly comparable, however In the case of the Urban Heat Island, it is reasonable to believe that spatial trends will be similar when comparing LST and air temperature, and therefore remotely sensed data is a useful dataset as absolute values are not vital in this methodology"*. However this research also contains an analysis to research the usability of Land Surface Temperature for the

research of the Urban Heat Island effect. For this analysis the map Stedelijk hitte-eiland effect (UHI) in Nederland will be used. The Stedelijk hitte-eiland effect map is the result of a model which calculates the average Urban Heat Island effect over the year by combining different datasets (Nationaal Georegister, 2022).

3.1.2 Air temperature

The Land Surface Temperature data will be compared with air temperature data to form a conclusion about the usability of Land Surface Temperature data. The reference air temperature data is collected from the RIVM which provides a map with the urban heat island effect based on several factors but mainly wind speeds and population density (Nationaal Georegister, 2022). The data shows the urban heat island effect as an average during the entire year, so it will not give the extreme values as expected from UHI data from a summer period but it will still be useful to see the correlation between air temperature data and LST data.

3.1.3 The BAG

Furthermore for this research data on the urban structure is used. One of the datasets contains different information of the buildings in the urban area. The data on buildings will be retrieved from the BAG which is the basisregistratie adressen en gebouwen in the Netherlands. It has all the information on different buildings in the Netherlands including the date the building was build (Kadaster, n.d.). Based on the BAG and the AHN Actueel Hoogtebestand Nederland a 3D dataset of the BAG is created. This dataset includes the height of each address and building in the Netherlands (tudelft3d, n.d.). This makes a possibility to also research hight in relation with the Urban Heat Islands. For the analysis the average age of the houses and the average building height in the neighbourhoods will be calculated.

3.1.4 Street Network

Also relevant for the research is the orientation of the street network of the corresponding neighbourhoods. The street network data will be selected on all modes of transport from OpenStreetMap. These are drive, bike and walk. This is done because some of the roads in city centres and neighbourhoods are prohibited for cars to drive in but are relevant for the analysis. So all transport types are selected to also include these parts of the network. With the network graph the network entropy will be calculated which tells something about the form of the street network. A high entropy value indicates that the street pattern has an organic layout. A low entropy value indicates that the street network has a more grid like pattern. From this network graph the orientation of the network can also be retrieved.

3.1.5 Water

The amount of water within the neighbourhood can be retrieved in multiple ways. The data set from the CBS from which the neighbourhoods and sub neighbourhoods are derived also contains the amount of water there is within each neighbourhood. It is also possible to use land use maps of the Netherlands from the CBS or a map of the BRT. For this research the neighbourhood and sub neighbourhood map from the CBS is used (CBS, 2022)

3.1.6 Vegetation

The amount of vegetation in the neighbourhood will be retrieved from the groenkaart of the Netherlands. The original maps shows the amount of green there is on a surface of 10 by 10 meters. Both trees, bushes and plants are taken into account as green. On the map areas with more green turn

darker on the map. Urban areas and especially industrial areas have a lighter colour. Agricultural areas do not show up as green in the dataset (RIVM, 2021).

The height of the vegetation can also be important for the UHI effect. Therefore a dataset containing all the trees in the Netherlands with their height is used in the analysis. This dataset is available on the internal hard drive of the Utrecht University.

3.1.7 Slope

The slope of the surfaces in the urban environment will also be taken into account. These attributes are derived from the Digital Terrain Model (DTM) which is calculated based on the AHN. For this research the DTM from the AHN3 is used. This is done because at the time of the research the DTM based on the AHN4 was not available for the entirety of the Netherlands. The city of Groningen which is part of the research area did not have a DTM model based on the AHN4. With the DTM the slope within the different cities can be calculated. The DTM used is made based on the Squared Inverse Distance Weighting method (Actueel Hoogtebestand Nederland, n.d.). With this method a value is calculated for each cell of 50 by 50 centimetres which contains the best value for the centre of the cell. Areas underneath buildings or water will receive a value of no-data. From this raster a new raster will be derived with a cell size of 5 metres filling in the gaps underneath the buildings by taking the average values of all the 50 by 50 centimetre cells falling within the area of the 5 meter cells (Actueel Hoogtebestand Nederland, n.d.).

3.1.8 Sky View Factor

Another metric which is derived from the AHN is the sky view factor. The sky view factor is calculated based on the Digital Surface Model based on the AHN 3. The Digital Surface Model based on the AHN can be downloaded from the ArcGIS online portal. There is the possibility to download the DSM with a 0.5 meter resolution or a 5 meter resolution (Esri Nederland, 2022). For this research the DSM with a resolution of 0.5 meters is used. This is done because it provides more detail which is especially of use when wanting to analyse on a sub-neighbourhood scale. Also the essence of the sky view factor regards narrow corners and steep edges between buildings and the surface of the streets which can be depicted better on a 0.5 meter resolution. The resulting sky view factor from the DSM will also be in a 0.5 meter resolution.

3.1.9 Low albedo surfaces

The data on surfaces with a low albedo will also be retrieved from the BGT. Here uses such as a road or parking lot will be used for the analysis because those will be made from asphalt which has a low albedo (Li, Harvey & Kendall, 2013). For this the total land surface of low albedo surfaces will be calculated in the neighbourhood. The total of low albedo surfaces will then be divided by the total area of the neighbourhood or sub neighbourhood to get the relative area of the low albedo surfaces.

3.2 Analysis

3.2.1 Research area

The research area of this study will be located in neighbourhoods in multiple cities in the Netherlands. These are neighbourhoods in Amsterdam, Rotterdam, Utrecht, Den Bosch, Groningen, Nijmegen and Maastricht. These cities are chosen because they are located all over the Netherlands, Maastricht in the south, Groningen in the north, Den Bosch and Utrecht more central, Nijmegen in the east and Rotterdam and Amsterdam in the western area of the Netherlands. With the locations more spread out a more generalist result can be expected from the research instead of a case study where the results only prove something on a single location. Also the urban form and structure is different between the cities. Where cities like Amsterdam and Den Bosch have an old historic build up the city

of Rotterdam is much newer. Also the cities of Rotterdam and Amsterdam feature more and diverse waterways while Nijmegen does have less. Also Nijmegen is located in a more sloped terrain when comparing it with the other cities. The variations in urban form and structures will also lead to a more generalized conclusion opposed to case study on one city. A map of the research area can be seen in the figure 2 below. Every city is shown in a different colour.

Figure 2, Research Area of this study



3.2.2 Data

The analysis done will be a multiple regression analysis between the urban structure variables and the relative surface temperature difference between the rural area and the neighbourhoods within the city. This will be done during the night and in the middle of the day where the skies are clear. This is done at the middle of the day because at that time the temperatures are the highest and most severe (Kraaijvanger, 2012). And during nights because the greatest differences occur between the temperature in rural areas and the urban environment (Klyzik and Fortunaik, 1999). Therefore this analysis will also be done for the temperatures during the night. The date chosen for the daytime data is the 11th of August in 2022 because this was a day when the skies were clear and the temperature was high. The maximum temperatures ranged from 26.3 degrees Celsius on the Waddeneilanden en

32.6 degrees Celsius in the south of the Netherlands in Noord-Brabant. The number of sun hours that day was 13.9 hours on average over the country (Weerplaats, 2022a). Another factor that influences the temperature in the city is the wind speed. The wind speed on the 11th of August 2022 were abstemious which makes it furthermore a useful day for this research (Persinfo, 2022). The night time images selected are from the 4th of July 2022. The images are taken between 03:45 and 03:50. This data is selected because there were less night images available with clear skies than the day images. The 4th of July was sunny summer day with maximum temperatures ranging from 20 to 25 degrees Celsius (Weerplaats, 2022b). The results will give more insights in the effect of the urban design on urban heat islands. However before this can be done the different variables and temperature values need to be calculated from the original datasets.

3.2.3 Land Surface Temperature

The value of the land surface temperature will be derived based on surface temperature of the roads within the boundaries of the neighbourhood. The land surface temperature of a neighbourhood will be calculated by retrieving the mean surface temperature based on the raster file generated from the ECOSTRESS land surface temperature. This raster file will be overlaid with the areas of the road segments within the neighbourhoods. This is done because outside at the road level there is more exposure to heat than in inside air conditioned environments (National Integrated Heat Health Information System, n.d.) . These road segments are retrieved from the BGT where a selection is made based on 'wegdeel' (BGT viewer, n.d.). The road segments are merged into one unified layer followed by a split based on the borders of the neighbourhoods. This is done so the road segments in each neighbourhood are accommodated with a table containing the right attributes from the neighbourhood such as the name and the code. At last the different layers are merged into one so the statistics on temperature can be calculated for them all at the same time. With the zonal statistics as a table function in ArcGIS pro the mean value will be calculated within the borders of the relevant road segments per neighbourhood. For the rural temperatures the mean temperature will be calculated for the road segments for a rural area next to the city. This will be done in the same way where the mean value of a patch of land will be calculated with the zonal statistics as table tool. Examples of the raster file retrieved from the ECOSTRESS thermal imagery can be seen below in figure 3. It shows the LST image of the 11th of August from the ECOSTRESS thermal instrument on Rotterdam. It is visible that the urban environment is of a lighter tone than the rural areas around it. The water is even darker. The darker the colour the lower the temperature measured by the instrument. Figure 4 shows the LST image of Den Bosch. Here the city is also visible as a lighter area compared to the rural area around it. Interesting in this image is that the rivers are white and warmer than the surface area over land. This is due to the time at which the image is taken. The image is taken at 03:47:50. At this time of the night the land had cooled of more than the water which takes longer to cool down than land area.

Figure 3, LST image of Rotterdam 11th of August 2022 during the day

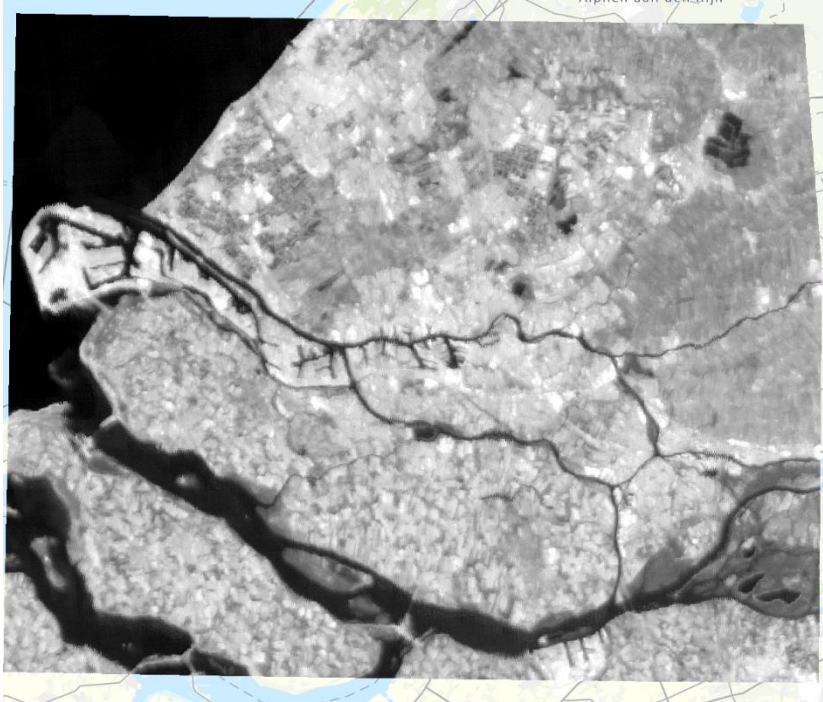
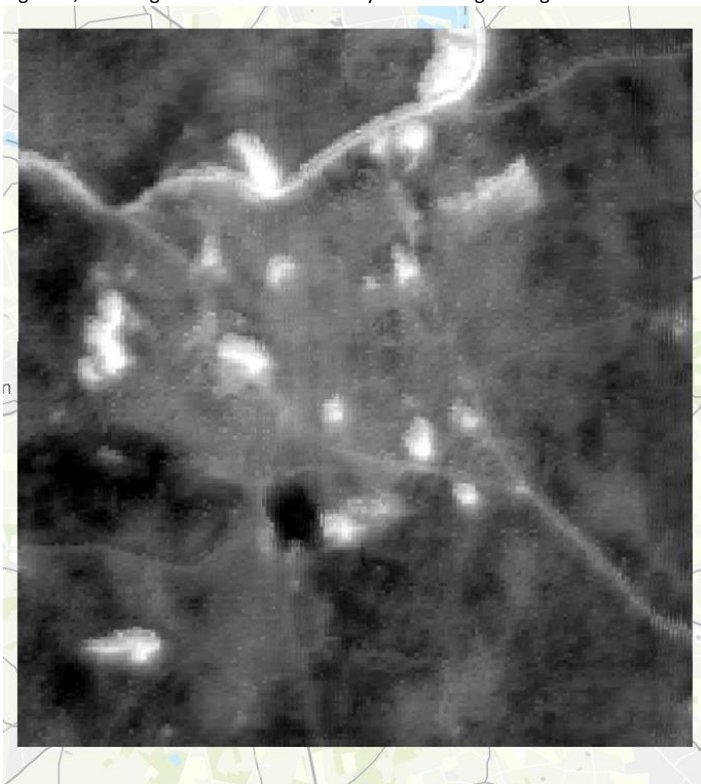


Figure 4, LST image of Den Bosch 4th of July 2022 during the night



3.2.4 Building age

The calculation for the age of buildings will be done according to the BAG. When loading the BAG data layer the matching table has different information on the buildings including the year they were built. The BAG dataset will be clipped with the neighbourhood layer of the research area and from this the median built year will be calculated. This means the middle value of all the buildings will be taken as the value into the analysis.

3.2.5 Building height

The height of buildings will be calculated quite similar. For this the 3D BAG will be loaded in and clipped with the relevant neighbourhood. The 3D BAG layer is equipped with the height of individual buildings. This feature layer will be turned into a raster so that it is able to be processed in the zonal statistics function. Another advantage of turning the data into a raster is that the larger buildings which likely have a larger influence are accounted for more in such a calculation. This is because the average height of buildings in the neighbourhood or sub neighbourhood is calculated by the average height per cell. When adding up all the heights of the building cells and dividing it by the number of building cells within the neighbourhood the average height of all buildings in the neighbourhood is calculated. This number can then be analysed in the regression.

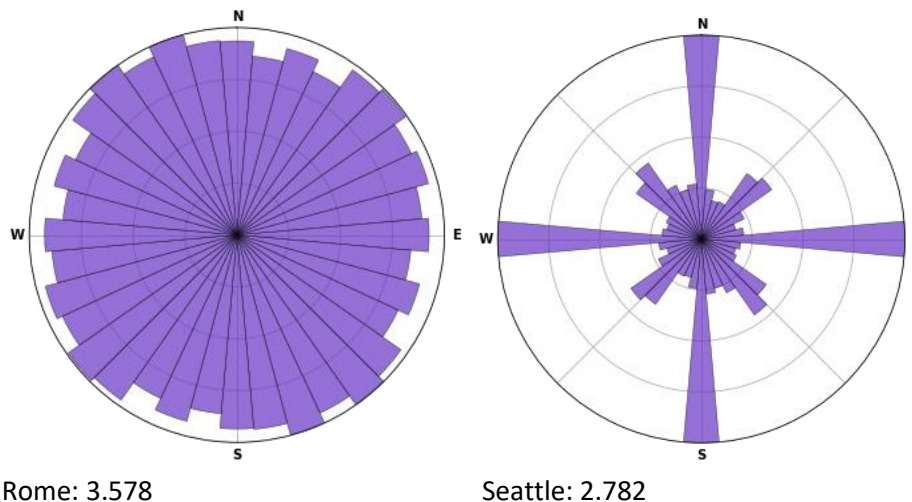
3.2.6 Entropy

Calculating the entropy of a street network has been done before and the method of Boeing et al (2019) will be followed. He divides the orientation of streets into 36 bins that each represent 10°. In his research he calculates the entropy of the streets orientation H as:

$$H_o = - \sum_{i=1}^n P(o_i) \log_e P(o_i)$$

Here n represents the number of bins, i is the bin index, and $P(o_i)$ the number of streets in bin i divided by the total number of streets. The lower the entropy the more of the streets fall into the same bin. The higher the entropy the more even the streets are distributed across all 36 bins. The minimum entropy is 0.693 and the maximum entropy 3.584 (Boeing et al 2019). The input for the entropy value calculation is the street network per neighbourhood derived from OpenStreetMap. In figure 5 two examples of results from the entropy calculation can be seen. The left image in the figure represents the street network of Rome and has an entropy value of 3.578. The image on the right represents the street network of the city of Seattle and has an entropy value of 2.782. This illustrates that a more organic street pattern where most of the shown circle is filled gives a high entropy value and a more grid like pattern where only parts of the shown circle are filled gives a lower entropy value.

Figure 5, Entropy graphs and values of Rome on the left and Seattle on the right.



3.2.7 Water surface

The amount of water in a neighbourhood will be calculated based on the BGT. Here a selection will be made with a layer consisting only of water as a result (BGT viewer, n.d.). It is also possible to retrieve the surface of water from a dataset from the TOP10NL. These datasets are part of the Basis Registratie

Topografie or BRT (pdok, n.d.). However a disadvantage of this dataset is that smaller water bodies with a maximum width of 6 meters are displayed as a line. This makes it impossible to calculate the area by the calculate geometry function. The water layer will be clipped with the outlines of the relative neighbourhood which results in a layer with all the water in the research area. The total surface of the water will then be divided by the total area of the neighbourhood. The result is a percentage of the neighbourhood which is covered by water.

3.2.8 Green

For the green area a raster map forms the basis of the data. The data within each neighbourhood will be calculated by the zonal statistics as table function. With this function the mean of all cells within the neighbourhood can be calculated for each neighbourhood. This will result in a table with an average percentage of the amount of green coverage for each neighbourhood.

Also relevant for the analysis is the height of the vegetation in this case the trees. The average height of the trees within each neighbourhood is calculated by dividing the total height of the trees by the number of trees within each neighbourhood. This can be done by the zonal statistics as table function. In this function the neighbourhoods define the borders of the zone and the number of points from the tree dataset is divided by the total height. This results in a table with the average tree height per neighbourhood.

3.2.9 Slope

The slope for each neighbourhood will be calculated by slope function in ArcGIS pro. This function identifies the slope for each cell based on an existing raster. The input raster is the DTM of the research area. Based on the height differences in the DTM the slope is calculated in percentage rise. This results in a new raster file containing slopes in a resolution of 0.5 by 0.5 meters. From this raster file the average slope in the neighbourhoods is calculated by the zonal statistics as table function.

3.2.10 Sky View Factor

The sky view factor is the fraction of visible sky from a certain point. When the sky view factor is close to one the short wave radiation reaches the surface without being blocked (Dirksen, Ronda, Theeuwes and Pagani, 2019). Within a more complex terrain reflection plays a role and the sky view factor will be lower than one. Within urban areas the complex structure of the 3D environment allows more opportunity for the absorption and emission of waves which reduces the value of the sky view factor (Dirksen et al, 2019). The figure used in the paper of Dirksen et al (2019) can give a clear overview and is seen and explained in figure 6. In the paper of Dirksen et al (2019) the sky view factor in a 2D and 3D space where in the 3D space a search radius of 100 meters and 16 different directions is good enough according to a paper from Dozier and Frew (1990).

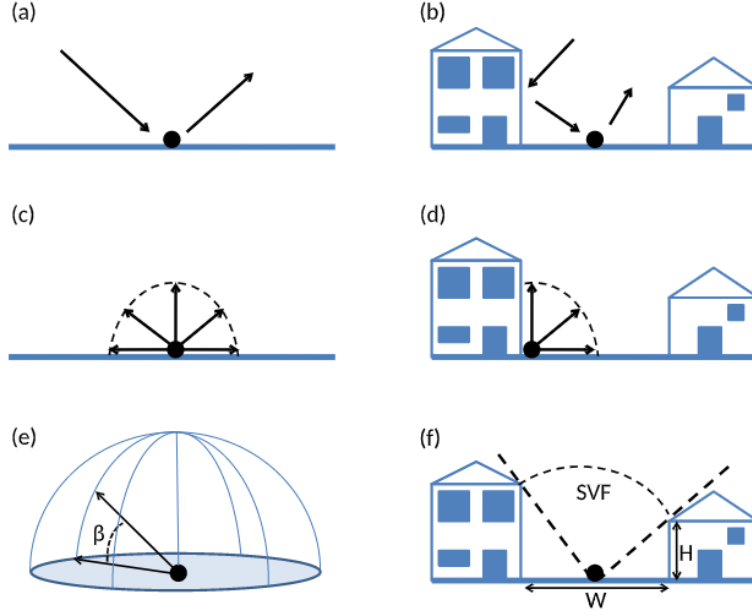


Figure 6. Radiation components given in an open field and street canyon and the illustration of sky view factor calculation. (a) Short wave radiation in an open field. (b) The path of short wave radiation in a street canyon. (c) The radiation of long waves in an open field. (d) Long wave radiation emission in a street canyon. (e) The sky view factor calculated in 3D, here β is the angle between the maximum obstacle height and the centre point. (f) Is the calculation of the sky view factor in 2D, here W is the street width and H is the building height. Figures are adapted from (Dirksen et al, 2019).

In this research a calculation will be made by computer for the 3D sky view factor. This is because in the urban environment corners and obstacles for radiation to travel can come from any direction and can be important regarding the temperatures. The sky view factor from a 3D perspective is calculated as follows for a point on a grid.

$$SVF = \int_{\theta=0}^{2\pi} \cos^2(\beta(R, \theta)) d\theta$$

Here β is the angle between the centre point for which the sky view factor will be calculated and the maximum obstacle height within a maximum distance which is equal to the constant search radius R . $d\theta$ gives the direction, when searching in all directions this value ranges from 0 to 2π , with this the sky view factor for the full hemisphere will be calculated. As said earlier a search radius of 100 meters and 16 different directions is good enough according to the paper of Dozier and Frew (1990). However the research of Dirksen et al (2019) concludes that a higher resolution in data and radius used results in smaller objects that are detected resulting in a better approximation. Within forest and city areas this impact is the largest (Dirksen et al, 2019). Therefore in the research the search radius will be increased to 500 meters and the maximum number of search sectors is selected. The result of the sky view factor analysis is a grid in the same resolution as the input raster. So for this research every cell of 0.5 by 0.5 meters contains the sky view factor value for the centre of that cell. Clipped out from this raster are the surfaces of buildings. This is because the structures of buildings often stand out above the urban environment on the street level which means the cells on top of buildings get a high sky view factor. When leaving the data points on top of the buildings in the calculation of the average sky view factor the value would be elevated whilst the data on the street level is most important for this research. After removing the buildings from the raster the raster layer of the sky view factor is overlaid with the neighbourhoods layer. From these layers the zonal statistics as table function will be performed. This results in an average sky view factor value per neighbourhood and sub neighbourhood. A raster as a result from the Sky View Factor calculation can be seen in figure 7. In this example the houses are already excluded from the data. The image in the figure shows the Sky View Factor data for the city of

Groningen. As seen in the image there are more white areas outside the city and more grey and dark areas within the city. The white areas show a higher Sky View Factor and the darker the cell the lower the Sky View Factor.

Figure 7, The Sky View Factor excluding buildings for the city of Groningen



3.2.11 Multi linear regression

All these different components that make up the urban environment will be used as the independent variables in a multi linear regression with the Urban Heat Island Effect based on Land Surface Temperature as the dependent variable. This analysis tests whether differences in urban design affect the land surface temperature on the streets. This analysis will only be conducted with the UHI data based on the LST during the day time. This is due to time constraints of the research and that the temperature values measured in this research are of a wider range during the day time than the night time. Also during the daytime people are more exposed to extreme heat (National Integrated Heat Health Information System, n.d.). The entropy value will be left out of the analysis for the sub neighbourhood scale because the entropy value is based on the street network within this entity. On the sub neighbourhood scale there is a majority of sub neighbourhoods which only consists of a few streets. When the sub neighbourhoods only have a few streets the entropy value is more likely to be high. This is because less streets make it less likely for an organic pattern to derive. A high entropy value might not be the case for the surrounding area as a whole which influence the area and the sub neighbourhood it is situated in.

3.2.12 Spatial Autocorrelation

Another analysis conducted during this research is to test if land surface temperature data from satellite imagery has the same characteristics in an urban environment as air temperature data. This will be tested by a Spatial Autocorrelation tool generating Moran's I which indicates if the LST is

dispersed random or clustered. It is widely known that in general air temperature has a high spatial correlation where high and low temperatures seem to cluster. This can also be seen in the research of Musashi, Pramoedyo and Fitriani (2018). This statistical test will result in a Moran's I value between -1 and 1 where -1 means there is a perfect clustering of dissimilar values, 1 means there is a perfect cluster of similar values and, 0 means there is no autocorrelation and the values are randomly dispersed over space (Statistics How To, n.d.). The results of this test will therefore show if the LST has one of the main characteristics of air temperature data.

3.2.13 Geographically weighted regression

Furthermore a geographically weighted regression will be done between the LST and air temperature to give insight into the possibility that the UHI effect calculated by LST correlate the UHI effect calculated by the air temperature. A geographically weighted regression is done because it incorporates the dependent and independent variables of the feature falling within the neighbourhood of each target feature (Esri, n.d.). So it not only checks if there is a correlation between the 2 values in the same neighbourhood but also checks the neighbourhoods and sub neighbourhoods around the feature. Especially on the sub neighbourhood scale this is relevant because these sub neighbourhoods are not as large and the resolution of the images from the ECOSTRESS instrument is 70 meters. So increasing the area in explaining the variable in the target feature can give accurate results. The geographically weighted regression results in an R-squared and an adjusted R-squared which gives the proportion of the dependent variable variance which is accounted for by the dependent variable, in this case the UHI data based on the LST. When setting up the model different settings and inputs are required. For neighbourhood type a selection is made for Distance band. This means that the neighbourhood is set as a constant or fixed distance for each feature. This is done because there is a difference in the size of the different neighbourhoods which should not matter for the temperature values. For the Neighbourhood Selection Method the Golden search method is selected. This is done because this method runs the model multiple times selecting the maximum and minimum number of neighbours and testing the model at various numbers. The Golden search method then determines the number of neighbours which generates the best model performance. For the Local Weighting Scheme the Gaussian method is chosen. This method gives weights to all features but the weights become exponentially smaller the further they get away from the target feature. This is done because it is expected that the temperature has a high spatial correlation and neighbouring neighbourhoods can have an effect on the targeted neighbourhood (Esri, n.d.).

3.3 Software

The data necessary for this research will mostly be handled within ArcGIS pro. This will mainly be for the preparation of the data but also a part of the analysis. The street network data will be gathered from Open Street Maps. This will be done using the OSMnx python package (Boeing, 2017). Streets with the network type "drive" will be gathered. Networks of this type only include roads that are destined for car travel. The networks entropy and orientation will be calculated with python. The calculation of the sky view factor will be done in SAGA this is a software designed for automated geoscientific analysis. It has a broad variability in tools but will only be used for calculating the sky view factor in this research. For the final analysis of the data the ordering will be done through excel. The statistical analysis will partly be done in ArcGIS pro and partly in SPSS. ArcGIS pro has the functionality to perform the spatial autocorrelation and the geographically weighted regression and SPSS has the functionality to perform the multiple linear regression.

3.4 Scope

With this research more insight will be given in the effect of different neighbourhood characteristics on Urban Heat Islands so further research can be done on the impact of surrounding neighbourhoods on the Urban Heat Island effect in the city centre. Also insight will be generated in the usability of satellite imagery for the research on UHI's. Therefore the impact of the urban design features which are the independent variables for this research will be compared with the UHI data from the LST recovered from a satellite and will not be compared with the UHI data based on the model from the RIVM based among other things on air temperature and wind speed.

4. Results

4.1 Spatial Autocorrelation

There are several analysis done within this research from which the results will be shown here. The results for the spatial autocorrelation of the Urban Heat Island effect based on the LST data are as follows. The analysis is split in four parts by the time and the scale. This analysis consists of the entire research area.

The map below shows the UHI effect based on LST during the day time in Groningen on a sub neighbourhood level. In the map you can see the Urban Heat Island effect becomes stronger the further you get into the city centre. The data shown in this map is part of the data used as input for the analysis.

Figure 8

UHI effect based on LST during the day time in Groningen

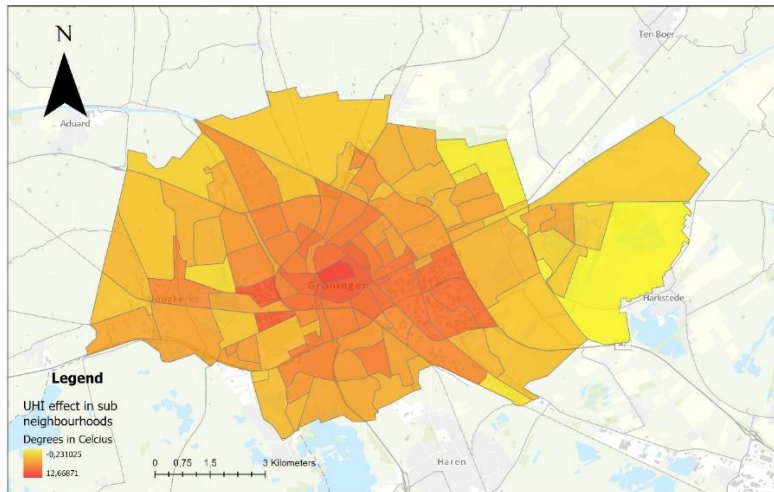
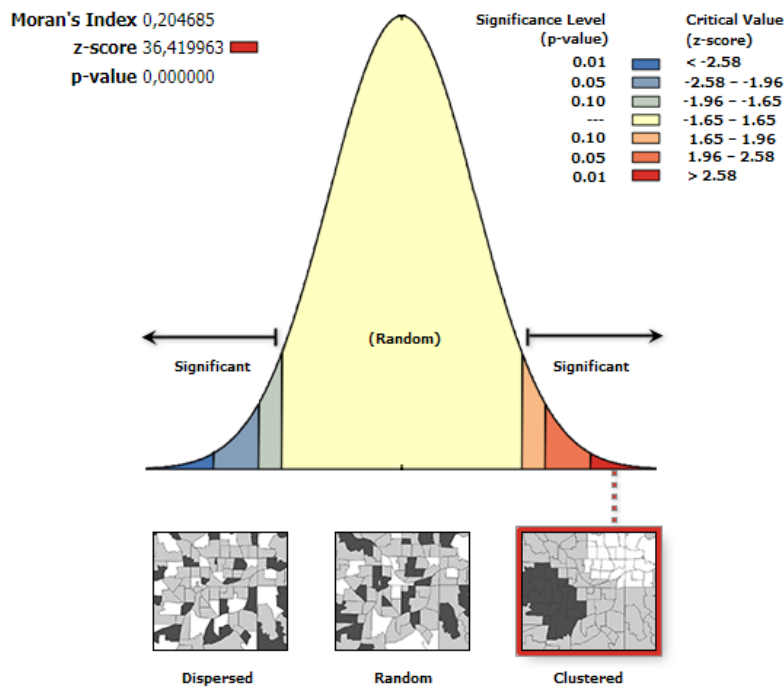


Figure 9 shows the results and show the higher temperature difference between the urban environment and the rural area are clustered on a sub neighbourhood scale. However before this can be stated the statistical significance needs to be guaranteed. For this analysis the z-score is 36.42 and the p-value is 0.000. This z-value indicates that the data is clustered in some way and the p-value shows that the model is significant. With the positive Moran's I of 0.205 this means there is a clustering of similar values.

Figure 9, Results of the spatial autocorrelation of the UHI effect from LST during the day on a sub neighbourhood scale.



The map below shows the UHI effect based on LST in Amsterdam on a neighbourhood scale during the day. In the map it shows that the outer areas of the Amsterdam areas show cooler than the neighbourhoods closer to the centre. Especially in Amsterdam West some warmer areas are clustered together.

Figure 10

UHI effect based on LST during the day time in Amsterdam

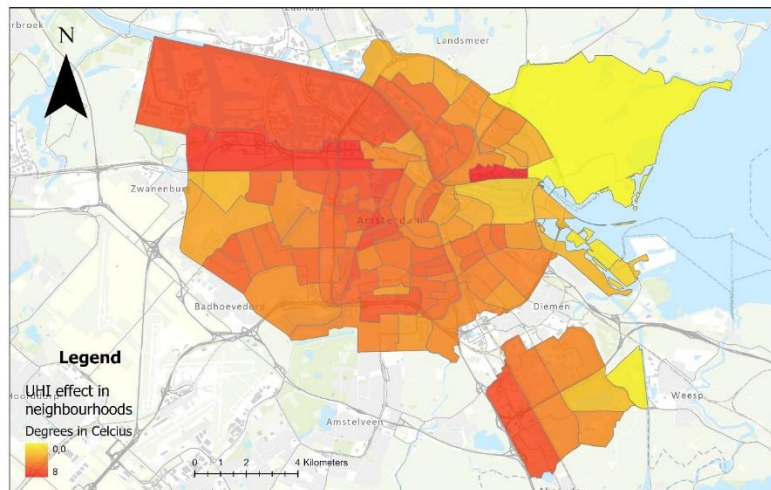
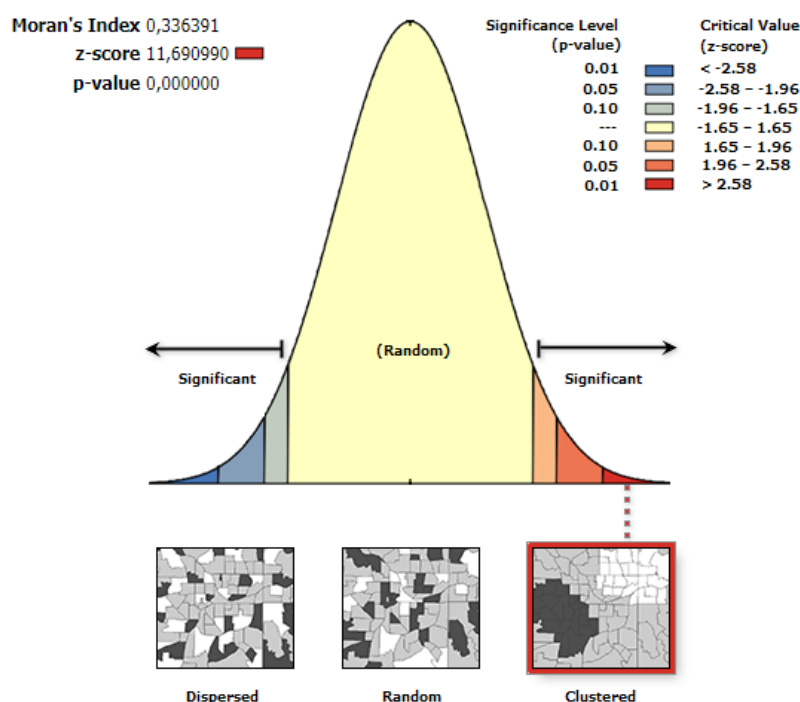


Figure 11 shows the results of the spatial autocorrelation of UHI data based on LST during the day on a neighbourhood scale. The figure shows that the temperature values are clustered in some form. The z-score is 11.69 and the p-value is 0.000. This means that the model is significant and there is clustering of some form. The Moran's I of 0.336 indicates that there is a clustering of similar values.

Figure 11, Results of the spatial autocorrelation of the UHI effect from LST during the day on a neighbourhood scale.



The map below shows the UHI effect based on LST in Rotterdam during the night on a sub neighbourhood scale. The map shows that during the night the warmer areas within the city are mainly located in the city centre and the harbour area. Within the harbour area and the city centre the LST is between 5 and 8.6 degrees warmer than the rural area around Rotterdam

Figure 12

UHI effect based on LST during the night time in Rotterdam

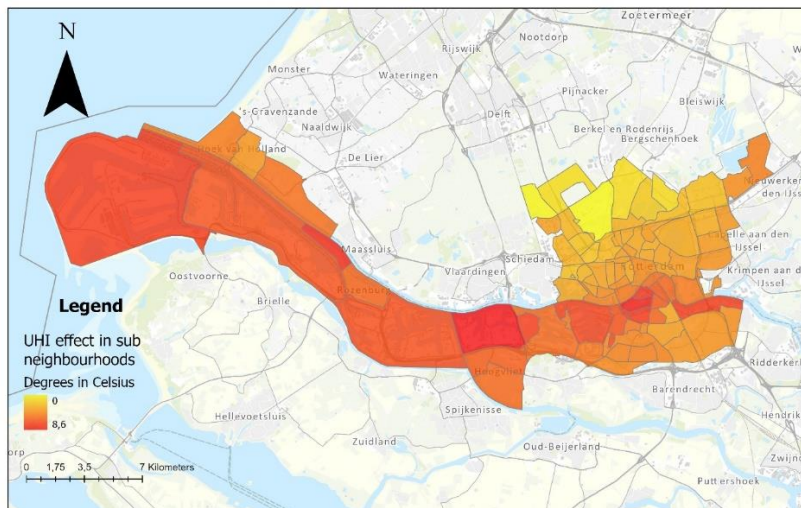
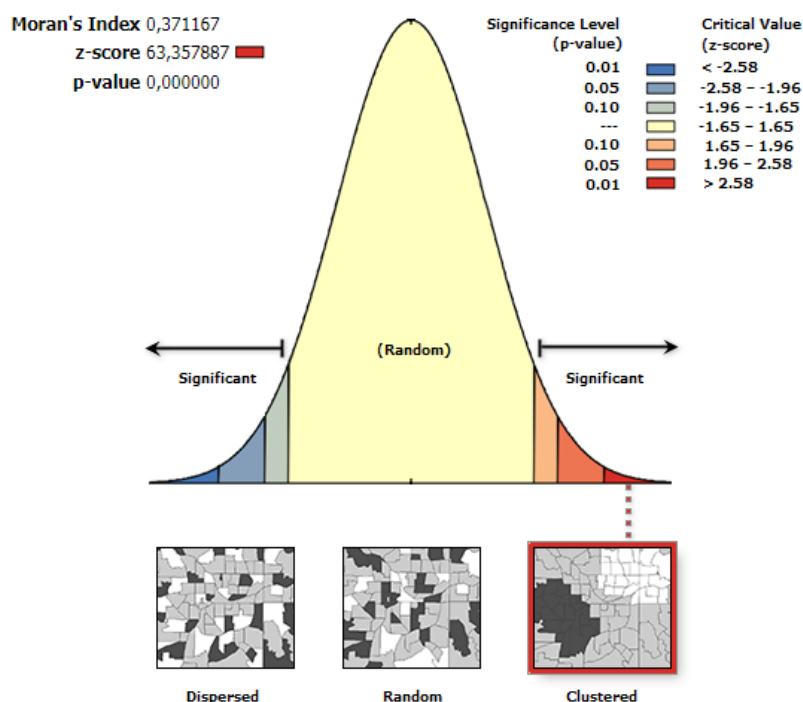


Figure 13 shows the results of spatial autocorrelation of the UHI effect from LST during the night on a sub neighbourhood scale. The figure shows that there is a clustering in the values. The z-score is 63.36 with a p-value of 0.000 this means that the model is significant and there is a clustered pattern within the research area. The Moran's I has a value of 0.371 which indicates that there is a clustering of similar values of the UHI effect from LST during the night time on a sub neighbourhood scale.

Figure 13, Results of the spatial autocorrelation of the UHI effect from LST during the night on a sub neighbourhood scale.



The map below shows the UHI effect based on the LST in Maastricht during the night time on a neighbourhood scale. What can be seen is that the city centre of Maastricht is warmer than the surrounding areas. However what also stands out is that the temperature difference between the city centre and the rural area around the city is only 1.9 degrees Celsius.

Figure 14

UHI effect based on LST during the night time in Maastricht

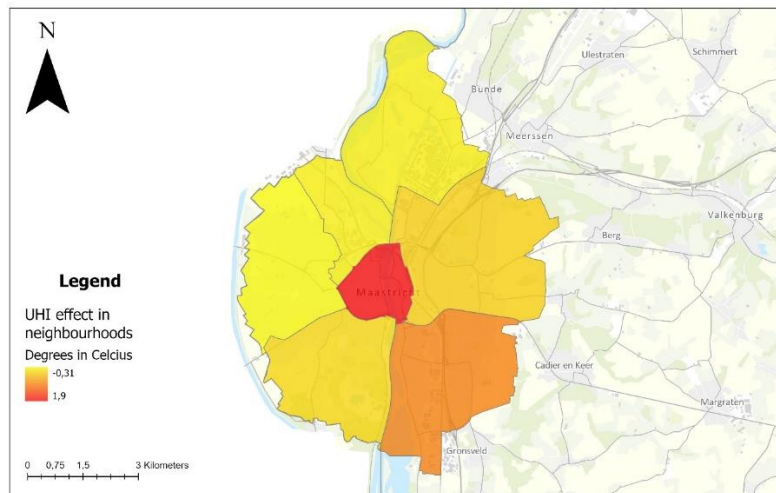
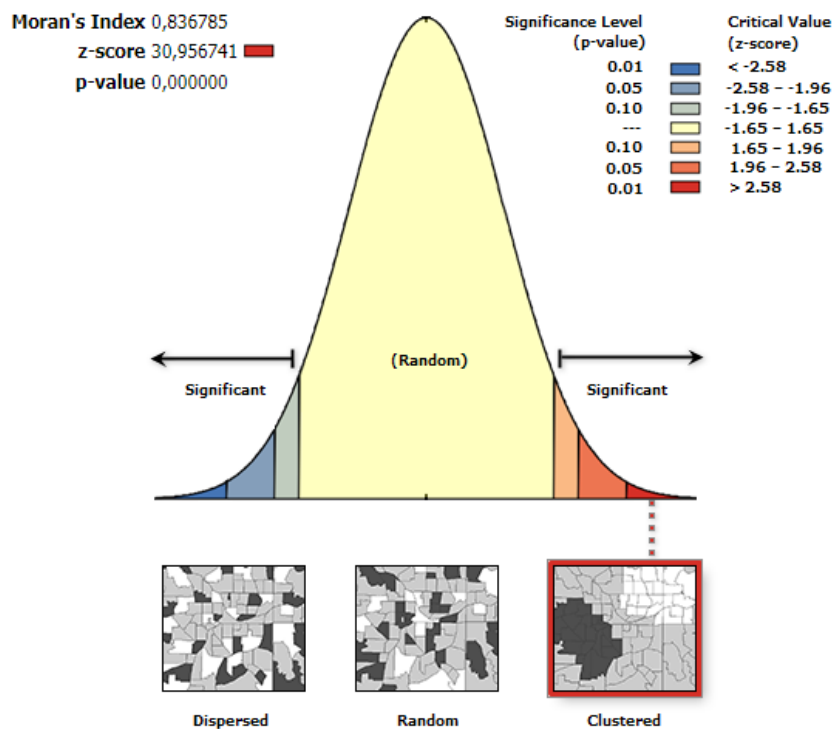


Figure 15 shows the results of the spatial autocorrelation of the UHI effect from LST during the night time on a neighbourhood scale. The model has a z-score of 30.96 with a p-value of 0.000 which indicates that the model is significant and there is a clustering of some sort. The Moran's I has a value of 0.837 which shows that there is a clustering within the research area of similar values of UHI data based on the LST during the night on a neighbourhood scale.

Figure 15, Results of the spatial autocorrelation of the UHI effect from LST during the night on a sub neighbourhood scale.



4.2 Geographically weighted regression

The results of the geographically weighted regression will be set out in four parts based on the time and neighbourhood type.

The results of the geographically weighted regression between the UHI data based on models of air temperatures and the UHI data based on the LST are as follows. These are the results of the LST during the day on a sub neighbourhood scale. For this model the R-squared is 0.91 and the adjusted R-squared is 0.89. This means that the dependent variable which is in this case the UHI based on the air temperature is for 89% accounted for by the independent variable which is the UHI effect based on the LST. The model is significant with $p < 0.01$ because the adjusted critical value of the pseudo t-statistic is larger than 2.58. The Pseudo-t statistic is 3.44. So based on the table Values of the t-distribution in the book of A. de Vocht (2019) the model is significant. The output table of the model can be found in figure 16.

Figure 16, Results of the Geographically weighted regression on a sub neighbourhood scale during day time.

Geographically weighted regression Model Diagnostics	Values
R2	0.9150
Adjusted R2	0.8910
AICc	-411.8718
Sigma-Squared	0.0330
Sigma-Squared MLE	0.0258
Effective Degrees of Freedom	763.8469
Adjusted Critical Value of Pseudo-T Statistics	3.4355

The results for the geographically weighted regression on a neighbourhood scale during the day time are as follows. The R-squared is 0.82 and the adjusted R-squared is 0.78. This means that the dependent variable of the UHI effect based on air temperature is for 78% accounted for by the UHI data based on the LST. The results of this model are significant $p < 0.01$ because the adjusted critical value of pseudo-t statistic is larger than 2.58. The pseudo-t statistic is 2.95. The output table of the model can be found in figure 16.

Figure 16, Results of the Geographically weighted regression on a neighbourhood scale during day time.

Geographically weighted regression Model Diagnostics	Values
R2	0.8216
Adjusted R2	0.7768
AICc	53.9188
Sigma-Squared	0.0669
Sigma-Squared MLE	0.0535
Effective Degrees of Freedom	140.0528
Adjusted Critical Value of Pseudo-T Statistics	2.9527

The model between the UHI data based on air temperature and the UHI data based on the LST on a sub neighbourhood scale during the night are as follows. The R-squared is 0.87 and the adjusted R-squared is 0.84. This means that within this model the dependent variable, the UHI data based on air temperature is for 84% accounted for by the independent variable which is the UHI data based on LST. The model is significant with $p < 0.01$ because the adjusted critical value of Pseudo-t statistic is larger than 2.58. The adjusted critical value of Pseudo-t statistic is 3.42. The output table of the model can be found in figure 17.

Figure 17, Results of the Geographically weighted regression on a sub neighbourhood scale during night time.

Geographically weighted regression Model Diagnostics	Values
R2	0.8765
Adjusted R2	0.8447
AICc	-80.3300
Sigma-Squared	0.0469
Sigma-Squared MLE	0.0373
Effective Degrees of Freedom	777.2798
Adjusted Critical Value of Pseudo-T Statistics	3.4151

The results of the geographically weighted regression on a neighbourhood scale during the night are as follows. The R-squared value is 0.64 and the adjusted R-squared value is 0.57. This means that 57% percent of the dependent variable which is the UHI effect based on the air temperature is accounted for by the independent variable of the UHI data based on LST. The model is significant with $p < 0.01$ because the adjusted critical value of the pseudo-t statistic is larger than 2.58. The pseudo-t statistic for this model is 2.92. The output table of this model can be found in figure 18.

Figure 18, Results of the Geographically weighted regression on a neighbourhood scale during night time.

Geographically weighted regression Model Diagnostics	Values
R2	0.6431
Adjusted R2	0.5655
AICc	170.6165
Sigma-Squared	0.1319
Sigma-Squared MLE	0.1085
Effective Degrees of Freedom	144.7767
Adjusted Critical Value of Pseudo-T Statistics	2.9197

Apart from the output table this analysis generates also plots of the relationship between the variables are made. These plots just show the relationship between the variables and are not geographically weighted. The different plots can be found in appendix 2 and 3.

4.3 Multiple linear regression

The multiple linear regression is done twice. Once with the UHI effect based on the LST during the day on a neighbourhood scale and once with the UHI effect based on the LST during the day on a sub neighbourhood scale. The UHI effect is the dependent variable and the Percentage of green, slope, building age, height of vegetation, the sky view factor, the surface area of the water, and low albedo surface area are the independent variables. For the UHI effect based on LST on a neighbourhood the entropy value is also included as an independent variable.

The results of the multiple linear regression between the mentioned variables in the method and the UHI effect based on LST on a sub neighbourhood scale are as follows. The R of the entire model is 0.59 which means that there is a strong relation between the dependent variable and the combination of independent variables. The R-squared of the model is 0.35 which means the model explains 35% of the variation in the UHI effect based on the LST. The adjusted R-squared is also 0.35 which means that the variation for the entire population, in this case the UHI effect based on the LST on a sub neighbourhood scale within all cities across the Netherlands is explained by 35%. The regression model in total is significant because $p < 0.001$. When looking at the results of the individual variables the following can be said. The variables; Percentage of green, the relative low albedo area, the relative surface area of water and the building height all have a significant effect on the dependent variable with $p < 0.01$. The percentage green and surface area of water have a negative effect on the UHI effect based on LST. The relative surface area of low albedo surfaces and the increased height of buildings have a positive effect on the dependent variable. Furthermore the median building age has a significant effect on the UHI effect based on LST with $p < 0.05$. The effect is negative, the newer the building the lower the UHI effect based on LST. The Sky View Factor, the height of the vegetation and the slope are insignificant in this model. The output tables resulting from this analysis can be found in figure 19.

Figure 19, Coefficients table as a result of the regression analysis between the UHI effect based on LST during the day and the independent variables on a sub neighbourhood scale.

Variables	Unstandardized B	Coefficients Std. Error	Standardized Coefficients Beta	t	Sig.
Constant	8.844	1.322		6.688	<0.001
Percentage of green	-0.050	0.005	-0.332	-9.415	<0.001
Slope	-0.039	0.066	-0.016	-0.599	0.550
median build year	-0.001	0.000	-0.059	-2.180	0.030
Hight green	0.051	0.094	0.015	0.541	0.589
Sky View Factor	-0.650	0.398	-0.048	-1.631	0.103
Relative low albedo surfaces	0.048	0.01	0.21	5.033	<0.001
Relative water surface area	-0.025	0.007	-0.116	-3.567	<0.001
Building height	0.044	0.014	0.098	3.204	0.001

When leaving out of the analysis the height of the vegetation and the low albedo surfaces the Sky View Factor becomes significant with $p < 0.01$. This can probably be due because the Sky View Factor itself can correlate with the height of the vegetation when the higher vegetation is blocking visible sky from the points the Sky View Factor is measured. Furthermore it is also possible that the Sky View Factor correlates with the relative amount of low albedo surfaces. This can be possible for example in on a narrow street where there is only space for the low albedo surface of the road with on both sides houses. When testing the correlation between the Sky View Factor and the height of the vegetation it turn out there is no significant correlation between the two variables. However when doing the same

for the Sky View Factor with the low albedo surfaces there is a significant correlation between the two variables $p < 0.001$. There is a strong correlation between the Sky View Factor and the relative amount of low albedo surfaces. The results of this correlation can be seen in figure 21. The results of the regression without the vegetation and low albedo surfaces are as follows and can be seen in figure 20. The R of the model is 0.57. This means there still is a strong correlation between the dependent and independent variables. The R-squared is 0.33 and the adjusted R-squared is also 0.33. This means that the variance of the dependent variable as well as the entire population is for 33% explained by the combination of independent variables. This regression model remains significant with $p < 0.001$.

Figure 20, Coefficients table as a result of the regression analysis between the UHI effect based on LST during the day and the independent variables minus the height of the vegetation and the relative amount of low albedo surfaces on a sub neighbourhood scale.

Variables	Unstandardized B	Coefficients Std. Error	Standardized Coefficients Beta	t	Sig.
Constant	11.666	0.967		12.060	<0.001
Percentage of green	-0.065	0.004	-0.438	-15.276	<0.001
Slope	-0.152	0.067	-0.021	-0.781	0.435
median build year	-0.001	0.000	-0.066	-2.435	0.015
Sky View Factor	-1.024	0.396	-0.077	-2.587	0.010
Relative water surface area	-0.042	0.006	-0.203	-6.881	<0.001
Building height	0.070	0.013	0.158	5.477	<0.001

Figure 21. Results of the correlation between the Sky View Factor and the relative amount of low albedo surfaces on a sub neighbourhood scale.

		Sky View Factor	Relative low albedo surfaces
Sky View Factor	Pearson Correlation	1	-0.398
	Sig. (2-tailed)		<0.001
	N	971	971
Relative low albedo surfaces	Pearson Correlation	-0.398	1
	Sig. (2-tailed)	<0.001	
	N	971	971

The results of the multiple linear regression between the mentioned variables above and the UHI effect based on LST on a neighbourhood scale are the following. The R of the model is 0.68. This means that there is a strong relationship between the dependent variables and the combination of independent variables. The R-squared of the model is 0.46. This means that the model explains 46% of the variance in the UHI effect based on the LST on a neighbourhood scale. The adjusted R-squared is 0.39. This means that the variation for the entire population, in this case the UHI effect based on LST on a neighbourhood scale for cities within the Netherlands is explained for 39% by this model. The regression model in total is significant because $p < 0.001$. When taking a look at the individual independent variables the percentage of green has a significant effect on the dependent variable $p < 0.01$. Also the relative surface area of water within the neighbourhood has a significant effect on the dependent variable $p < 0.05$. Both the regression variables of these independent variables are negative. This means that when the percentage of green or the relative amount of water within the neighbourhood increases the UHI effect based on LST decreases. The other independent variables; The Sky View Factor, the relative surface area of low albedo surface, the entropy, building age, height of the buildings, height of vegetation and slope all have an insignificant effect on the UHI effect based on LST within this model. The table of the results can be seen below in figure 22.

Figure 22 , Coefficients table as a result of the regression analysis between the UHI effect based on LST during the day and the independent variables on a neighbourhood scale.

Variables	Unstandardized B	Coefficients Std. Error	Standardized Coefficients Beta	t	Sig.
Constant	8.511	3.841		2.215	0.030
Percentage of green	-0.084	0.017	-0.707	-4.854	<0.001
Slope	-0.126	0.166	-0.075	-0.755	0.452
median build year	0.002	0.002	0.136	1.098	0.276
Hight green	0.083	0.158	0.057	0.524	0.602
Sky View Factor	-0.766	1.106	-0.083	-0.693	0.491
Relative low albedo surfaces	-0.033	0.018	-0.273	-1.814	0.074
Relative water surface area	-0.032	0.013	-0.281	-2.568	0.012
Building height	0.009	0.57	0.021	0.163	0.871
Entropy	-0.672	0.453	-0.146	-1.484	0.142

Per variable the reason they are insignificant can be different. For the slope it is probably due that the research area within the Netherlands is mainly flat and there is little difference in slope between the different neighbourhoods. The entropy value is insignificant due to the little input values the variable has. Only for 86 neighbourhoods the entropy value could be calculated. The height of the green also turned out to be insignificant in the regression analysis on a sub neighbourhood scale. This is probably because the height of the vegetation does not effect the temperature on the surface. The other variables; The Sky View factor, the relative surface area of low albedo surfaces, the building age and height of the buildings were significant on a sub neighbourhood scale but not on the neighbourhood scale. This can be due to the lesser amount of input in the analysis, 176 features on the neighbourhood scale and 986 on the sub neighbourhood scale. Another explanation is that the neighbourhood division as made by the CBS is to large for the analysis. As seen in the map below the city of Utrecht only consists of 10 individual neighbourhoods according to the dataset of the CBS. These larger neighbourhoods even out the average of the different indicators. For example some parts of the neighbourhood have higher buildings and more low albedo surfaces whilst other parts have lower buildings and les low albedo surfaces. The differences within the same neighbourhood even out the input numbers into the regression. This is a probable reason that some of the variables which showed significant on the sub neighbourhood scale are insignificant on the neighbourhood scale. A map of the research area zoomed in on Utrecht is seen in figure 23 below.

However for some variables which are closer to a level of significance of $p < 0.05$ become of significant impact on the dependent variable when some other independent variables are left out. For example the entropy value becomes significant with $p < 0.05$ when it is in the model with only the relative water surface area and the percentage of green in the neighbourhood. The results of the linear regression analysis with UHI based on LST during the day as the dependent variable and the entropy value, Relative water surface area and the percentage of green as the independent variables are the following. The R is 0.653 which means there is a strong correlation between the dependent variable and the combination of independent variables. The R square is 0.43 and the adjusted R square is 0.41. This means that that 46% of the difference in the dependent variable is explained by the independent variables and that 41% of difference in the entire population is explained by the independent variables. Furthermore the model is significant with $p < 0.001$. The results of the individual variables can be seen in figure 24 below.

Figure 23, The neighbourhood configuration in Utrecht according to the CBS.

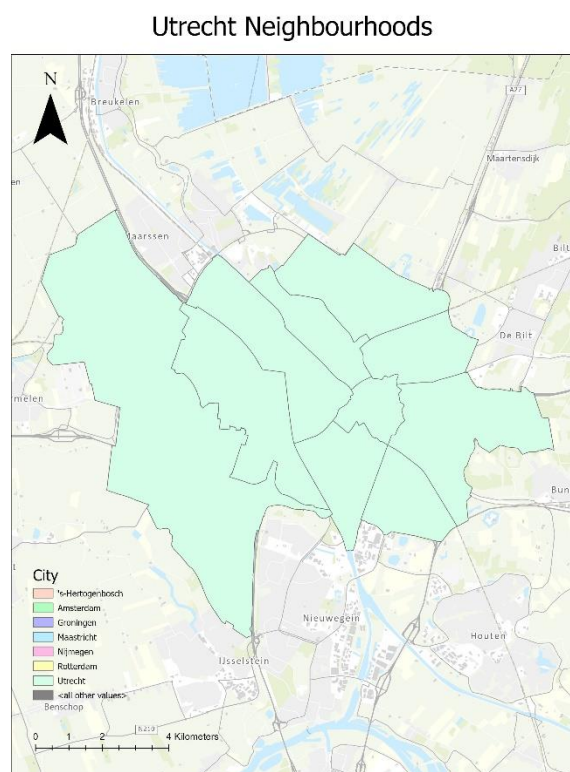


Figure 24, Coefficients table as a result of the regression analysis between the UHI effect based on LST during the day and the independent variables; percentage of green, relative water surface area and entropy on a neighbourhood scale.

Variables	Unstandardized B	Coefficients Std. Error	Standardized Coefficients Beta	t	Sig.
Constant	11.332	1.251		9.057	<0.001
Percentage of green	-0.061	0.011	-0.515	-5.718	<0.001
Relative water surface area	-0.026	0.01	-0.224	-2.644	0.010
Entropy	-0.981	0.431	-0.206	-2.277	0.025

5. Conclusion

When looking back at the research question formulated at the beginning of this research with the corresponding hypothesis the following can be said. The analysis showed that the usage of thermal sensors mounted to a satellite can generate LST images and values which can be used for the analysis of Urban Heat Islands. The UHI data generated from the LST on both the sub neighbourhood scale as well as the neighbourhood scale showed significant positive correlation with the Urban Heat Island data derived from a model based on air temperatures. For both the data derived at the middle of the day as well as the data derived from the night the results were positive. However the results during the day time explained more of the variance of the Urban Heat Island effect based on air temperature than the results during the night time. This can be due to the lower temperatures values derived during the night time in comparison to the day time which can result in smaller differences in temperature between the urban environment and surrounding rural area. Therefore it can be said that the use of thermal imagery for research into Urban Heat Island can especially be helpful during clear warm days. At these days the UHI effect based on LST will be the most similar to the UHI effect based on the air temperature. These results correspond with hypothesis number one which expected that the LST based on satellite imagery can be a useful tool in mapping the Urban Heat Island effect at different circumstances. The results from this research show that at the different tested circumstances, day and night the UHI data based on LST significantly matched with the UHI data based on air temperature models.

With the results of the multiple linear regression the following can be said about the indicators and urban design features that have an influence on Urban Heat Islands as measured using the LST. On the neighbourhood level only the percentage of green in the neighbourhood and the relative surface area of water are significant and have an influence on the Urban Heat Island effect. They both have a negative effect on the Urban Heat Island effect based on LST. This corresponds with hypothesis number 3. On a sub neighbourhood level the Percentage of green in the area, the building age, the building height, the relative amount of low albedo surfaces and the relative amount of water in the area all have a significant effect on the UHI effect based on LST. After further research and testing it turned out that in certain situation also the entropy value and Sky View Factor were significant as an indicator explaining the UHI effect based on LST during the day. For the Entropy value this is on a neighbourhood scale and the Sky View Factor is significant on a sub neighbourhood scale. The difference in significant indicators can be due to the scale of measurement. Most of the indicators are calculated as an average in the neighbourhood which means that more extreme values get evened out over space. On the neighbourhood scale this effect is larger than on a sub neighbourhood scale. In combination with number of neighbourhoods compared with the number of sub neighbourhoods 176 vs 986 it is more likely to get significant results on a sub neighbourhood level. The percentage of green, the building age, the entropy, the Sky View Factor and the relative surface area of water have a negative relation with the UHI effect. The relative amount of low albedo surfaces and the average height of buildings have positive relation with the UHI effect. These findings correspond with hypothesis 2 and 3. The height of the vegetation and slope had no significant effect in any of the multiple linear regression models. This contradicts Hypothesis number 2 and 3 because it was expected that these variables would have a significant effect on Urban Heat Islands. No correlation between the UHI effect and the slope can be explained by the fact that the majority of the Netherlands is flat which makes the differences between the different neighbourhoods and sub neighbourhoods minimal which makes getting a significant result harder.

So to come back on the main research question; What urban design features in different neighbourhoods of cities within the Netherlands have an influence on Urban Heat Islands over time? The following can be stated. Most of the tested urban design features had an effect on the UHI effect

based on LST in some form. Urban design features like vegetation and water in the area influence the UHI effect and decrease the UHI effect. When minimizing the amount of low albedo surfaces the UHI effect can also be decreased. Also neighbourhoods within the research area with newer houses decrease the severity of the UHI effect. The average height of the buildings should remain low to minimize the UHI effect. When the Sky View Factor is higher the UHI effect decreases. So increasing the amount of visible sky within a neighbourhood and keeping an open structure should decrease the UHI effect. At last the entropy value. A higher entropy value will decrease the UHI effect within a neighbourhood. So a more organic street pattern will result in a lesser UHI effect and a more grid like street pattern will increase the UHI effect.

6. Discussion

Within this research there are some points of discussion regarding the input data and the results.

6.1 Entropy values

The entropy value based on the road network in neighbourhoods of the city is calculated with the street network from OpenStreetMap. OpenStreetMap is a map of the world with an accuracy based on the input of its users. As a user you are able to make an account and adjustments to the map, This makes the application more vulnerable to little errors. During the research it was also discovered that the boundaries used by OpenStreetMap for neighbourhoods and sub neighbourhoods in the Netherlands sometimes differ from the neighbourhood and sub neighbourhood structure used by the CBS. This was especially the case in the city of Utrecht where none of the neighbourhoods matched between the datasets. Therefore the entropy value could not be taken into account for the analysis for those areas.

Furthermore during the research when taking a closer look at the street networks within the sub neighbourhood they often consist of just a few streets which make the entropy value very low. This would often give an incorrect view when combining the sub neighbourhood with its surroundings. Therefore the Entropy value is left out of the multiple linear regression model on the sub neighbourhood scale.

6.2 Sky view factor

Something that was eye catching when analysing the sky view factor data is that underneath and near trees the value is one of the lowest in the analysis. However, it is expected that a lower value of the sky view factor will result in higher temperatures, opposed to that the expectation around green is that whenever there is more green in the area the temperature would decrease. The effect of trees on the lower sky view factor could have an effect on the results of this research.

6.3 Slope and Aspect

It was planned for this research to include the aspect and slope into the multiple linear regression models of this research. The slope was included within the regression model however because this analysis is done within the Netherlands the variable was insignificant within the model. When zooming into the data only a few neighbourhoods within Nijmegen have a unanimous slope greater than a few degrees. With this little input it is on no surprise that the variable turned out to be insignificant. If the study area had more sloped or mountainous terrain the results could be different. These factors also play a role in the aspect within the neighbourhoods. However the aspect has also other difficulties regarding being the input for the multiple linear regression model. The aspect is a dichotomous variable which means it can not be used as the input for a regression. The variable could be used as the input when dummy variables are created. However because the aspect had many different values like; north, north east, east, south east and so forth which would make creating dummy variables a lot harder and the slope within the research area already turned out to be insignificant. Therefore it is chosen to leave out the aspect of the multiple linear regression models.

6.4 Results

There are also some points of discussion regarding the results of this research. Expected was that the Sky View Factor, the height of the green and entropy value would immediately be significant in the multiple linear regression analysis within this research. The Sky View Factor was not significant in the regression models first run in this research. However when removing the low albedo surfaces as a variable or when running a linear regression only with the Sky View Factor as the independent variable

the variable becomes significant. Therefore the Sky View Factor is still a relevant variable in explaining the UHI effect based on LST. However more research into the effect of the Sky View Factor in combination with other urban features should be conducted and can be useful to get a better understanding of combining different urban features.

The entropy value is most probably insignificant in the first runs because the script used for calculating the entropy value did not recognize all the neighbourhoods. Therefore the number of inputs is only 86 features which generally could decrease the significance of the variable within statistical tests. Also the multiple linear regression model on the neighbourhood scale only consisted of 176 items. This can be sufficient for some significant results however a higher number of items will increase the strength of the model. However when removing some initially insignificant variables the entropy of the street network becomes significant within the model. Relevant for this research should be to expand the number of neighbourhoods and make sure that the entropy value can be calculated for all of them. This will probably give an initially more convincing result with the current knowledge that the entropy already has a significant impact on the UHI effect based on LST.

6.5 Recommendations

The results from the spatial autocorrelation and the geographically weighted regression showed that thermal imagery from instruments mounted to satellites can well be used in the research into Urban Heat Islands. However, the results from this research only show the effectivity of the instruments on certain moments. Results from the night time on a less warm day already showed lesser explained variances. However these were still high for these tests. Also during clouded days these instruments become useless in collecting surface temperatures. However maybe a drone or small plane flying below the clouds could provide necessary data. So recommended is to do further research on the possibilities of using LST in providing UHI data during other periods of the year than the clear and warmest summer days.

Also expanding the research area to include more neighbourhoods and other countries where the slope and aspect could have an influence on the UHI effect would be good for further understanding how these factors explain the variance in the UHI effect based on LST. Furthermore keeping the different entities, in this research the neighbourhoods and sub neighbourhoods small. Larger entities can cancel out the values of some of the indicators.

Regarding recommendations for future policy. Important factors to take into account when designing new neighbourhoods and cities is that Urban Heat Island testing can be done using surface temperatures. The characteristics of higher buildings and more low albedo surfaces will increase the UHI effect and should be minimized whilst more water surface area and more green within a neighbourhood will decrease the UHI effect. A good balance between the significant characteristics from this research should be sought after when designing new urban environments.

7. Literature

- 3D geoinformation research group. (n.d.). *Overzicht - 3D BAG*. Retrieved October 12, 2022, from <https://docs.3dbag.nl/nl/>
- Actueel Hoogtebestand Nederland*. (n.d.). 5. Producten. AHN. <https://www.ahn.nl/5-producten>
- Agirbas, A., & Ardaman, E. (2017). Macro-scale designs through topological deformations in the built environment. *International Journal of Architectural Computing*, 15(2), 134–147. <https://doi.org/10.1177/1478077117714915>
- AHN3 - Download kaartbladen*. (2015). [Dataset; ArcGis Online]. Esri Nederland. <https://www.arcgis.com/home/item.html?id=9039d4ec38ed444587c46f8689f0435e>
- Akbari, H., & Rose, L. S. (2008). Urban surfaces and heat island mitigation potentials. *Journal of the Human-environment System*, 11(2), 85-101.
- BAG viewer*. (n.d.). Retrieved October 12, 2022, from <https://bagviewer.kadaster.nl/lvbag/bag-viewer/index.html>
- BGTviewer - de Basisregistratie Grootchalige Topografie op de kaart*. (n.d.). <https://bgtviewer.nl/info/over>
- Boeing, G. (2017). OSMnx: New Methods for Acquiring, Constructing, Analyzing, and Visualizing Complex Street Networks. *Computers, Environment and Urban Systems* 65, 126-139. doi:10.1016/j.compenvurbsys.2017.05.004
- Boeing, G. (2019). Urban spatial order: street network orientation, configuration, and entropy. *Applied Network Science*, 4(1), 1–19. <https://doi.org/10.1007/s41109-019-0189-1>
- Cawse-Nicholson, K. (n.d.). *ECOSTRESS demo* [Slide show; PowerPoint]. [ecostress.nasa.gov. https://ecostress.jpl.nasa.gov/downloads/other/ECOSTRESS_demo.pdf](https://ecostress.jpl.nasa.gov/downloads/other/ECOSTRESS_demo.pdf)
- CBS. (2022). *Wijk- en buurtkaart 2022*. Centraal Bureau Voor De Statistiek. <https://www.cbs.nl/nl-nl/dossier/nederland-regionaal/geografische-data/wijk-en-buurtkaart-2022>
- Chang, Y., Xiao, J., Li, X., Middel, A., Zhang, Y., Gu, Z., ... & He, S. (2021). Exploring diurnal thermal variations in urban local climate zones with ECOSTRESS land surface temperature data. *Remote Sensing of Environment*, 263, 112544.
- Dataset: Basisregistratie topografie (BRT) TOPNL*. (2022). [Dataset]. pdok. <https://www.pdok.nl/introductie/-/article/basisregistratie-topografie-brt-topnl>
- Dirksen, M., Ronda, R. J., Theeuwes, N. E., & Pagani, G. A. (2019). Sky view factor calculations and its application in urban heat island studies. *Urban Climate*, 30, 100498.
- Dozier, J., & Frew, J. (1990). Rapid calculation of terrain parameters for radiation modeling from digital elevation data. *IEEE Transactions on geoscience and remote sensing*, 28(5), 963-969.
- Esri. (n.d.). *How Geographically Weighted Regression (GWR) works—ArcGIS Pro | Documentation*. <https://pro.arcgis.com/en/pro-app/latest/tool-reference/spatial-statistics/how-geographicallyweightedregression-works.htm>
- Heat Island Impacts*. (2022, September 2). US EPA. Retrieved October 12, 2022, from <https://www.epa.gov/heatislands/heat-island-impacts>
- Hook, S. J., Cawse-Nicholson, K., Barsi, J., Radocinski, R., Hulley, G. C., Johnson, W. R., ... & Markham, B. (2019). In-flight validation of the ECOSTRESS, Landsats 7 and 8 thermal

- infrared spectral channels using the Lake Tahoe CA/NV and Salton Sea CA automated validation sites. *IEEE Transactions on Geoscience and Remote Sensing*, 58(2), 1294-1302.
- Howard, L. (2012). *The climate of London: deduced from meteorological observations* (Vol. 1). Cambridge University Press.
- Hulley, G. C., Göttsche, F. M., Rivera, G., Hook, S. J., Freepartner, R. J., Martin, M. A., ... & Johnson, W. R. (2021). Validation and quality assessment of the ECOSTRESS level-2 land surface temperature and emissivity product. *IEEE Transactions on Geoscience and Remote Sensing*, 60, 1-23.
- Khan, A., Chatterjee, S., & Wang, Y. (2020). *Urban Heat Island Modeling for Tropical Climates*. Elsevier.
- Khemet, B., & Richman, R. (2018). A univariate and multiple linear regression analysis on a national fan (de) Pressurization testing database to predict airtightness in houses. *Building and Environment*, 146, 88-97.
- Kraaijvanger, T. (2012, September 7). *Meteorologie: zeven vragen, zeven antwoorden*. Scientias.nl. <https://scientias.nl/meteorologie-zeven-vragen-zeven-antwoorden/#:~:text=Hoewel%20de%20zon%20het%20hoogst,eerder%20of%20later%20worden%20bereikt>
- Klysik, K., & Fortuniak, K. (1999). Temporal and spatial characteristics of the urban heat island of Łódź, Poland. *Atmospheric environment*, 33(24-25), 3885-3895.
- Li, H., Harvey, J., & Kendall, A. (2013). Field measurement of albedo for different land cover materials and effects on thermal performance. *Building and environment*, 59, 536-546.
- Li, Z. L., Tang, B. H., Wu, H., Ren, H., Yan, G., Wan, Z., ... & Sobrino, J. A. (2013). Satellite-derived land surface temperature: Current status and perspectives. *Remote sensing of environment*, 131, 14-37.
- Li, Z. L. L., A Sobrino, J. A. S., & Song, X. S. (n.d.). *Remote Sensing*. https://www.mdpi.com/journal/remotesensing/special_issues/thermal-infrared
- Low-Rise Building*. (n.d.). FEMA.gov. Retrieved October 12, 2022, from <https://www.fema.gov/node/404816>
- Lynch, K., & Hack, G. (1984). *Site Planning*(3rd ed.). MIT Press.
- Margaritis, E., & Kang, J. (2016). Relationship between urban green spaces and other features of urban morphology with traffic noise distribution. *Urban Forestry and Urban Greening*, 15, 174–185. <https://doi.org/10.1016/j.ufug.2015.12.009>
- Masson, V., Lemonsu, A., Hidalgo, J., & Voogt, J. (2020). Urban climates and climate change. *Annual Review of Environment and Resources*, 45, 411-444.
- Mohajerani, A., Bakaric, J., & Jeffrey-Bailey, T. (2017). The urban heat island effect, its causes, and mitigation, with reference to the thermal properties of asphalt concrete. *Journal of environmental management*, 197, 522-538.
- Musashi, J. P., Pramoedyo, H., & Fitriani, R. (2018). Comparison of inverse distance weighted and natural neighbor interpolation method at air temperature data in Malang region. *CAUCHY: Jurnal Matematika Murni dan Aplikasi*, 5(2), 48-54.
- NASA. (n.d.). *About NASA*. NASA. <https://www.nasa.gov/about/index.html>

Nationaal georegister. (n.d.).

<https://nationalegeoregister.nl/geonetwork/srv/dut/catalog.search#/metadata/c9aa9109-3f32-4f65-84e5-bb1c9ebdfbec?tab=general>

Nationaal georegister. (2022, December 16).

<https://nationalegeoregister.nl/geonetwork/srv/dut/catalog.search#/metadata/c9aa9109-3f32-4f65-84e5-bb1c9ebdfbec?tab=general>

Nichol, J. (2005). Remote sensing of urban heat islands by day and night. *Photogrammetric Engineering & Remote Sensing*, 71(5), 613-621.

Nuruzzaman, M. (2015). Urban heat island: causes, effects and mitigation measures-a review. *International Journal of Environmental Monitoring and Analysis*, 3(2), 67-73.

Oke, T. R. (1982). The energetic basis of the urban heat island. *Quarterly Journal of the Royal Meteorological Society*, 108(455), 1-24.

Paravantis, J., Santamouris, M., Cartalis, C., Efthymiou, C., & Kontoulis, N. (2017). Mortality associated with high ambient temperatures, heatwaves, and the urban heat island in Athens, Greece. *Sustainability*, 9(4), 606.

Persinfo. (2022, August 11). *HET WEER : donderdag 11 augustus – veel zon en warm*. Persinfo. <https://www.persinfo.org/nl/nieuws/artikel/het-weer-donderdag-11-augustus-veel-zon-en-warm/53158>

Rajagopalan, P., Lim, K. C., & Jamei, E. (2014). Urban heat island and wind flow characteristics of a tropical city. *Solar Energy*, 107, 159-170.

Ramamurthy, P., & Bou-Zeid, E. (2017). Heatwaves and urban heat islands: a comparative analysis of multiple cities. *Journal of Geophysical Research: Atmospheres*, 122(1), 168-178.

Rieke, C. (2021, August 1). *Thermal imaging with satellites - Christoph Rieke*. Medium. Retrieved October 19, 2022, from <https://chrieke.medium.com/thermal-imaging-with-satellites-34f381856dd1>

RIVM. (n.d.). Atlas Leefomgeving. <https://www.atlasleefomgeving.nl/groenkaart-van-nederland>

Santamouris, M. (2013). *Energy and climate in the urban built environment*. Routledge.

Santamouris, M. (2015). Analyzing the heat island magnitude and characteristics in one hundred Asian and Australian cities and regions. *Science of the Total Environment*, 512, 582-598.

Statistics How To. (n.d.). *Moran's I: Definition, Examples - Statistics How To*. Statistics How To. <https://www.statisticshowto.com/morans-i/#:~:text=What%20is%20Moran's%20I%3F,the%20observations%20are%20not%20independent.>

Steeneveld, G. J., Koopmans, S., Heusinkveld, B. G., & Theeuwes, N. E. (2014). Refreshing the role of open water surfaces on mitigating the maximum urban heat island effect. *Landscape and Urban Planning*, 121, 92-96.

Stewart, I. D. (2019). Why should urban heat island researchers study history?. *Urban Climate*, 30, 100484.

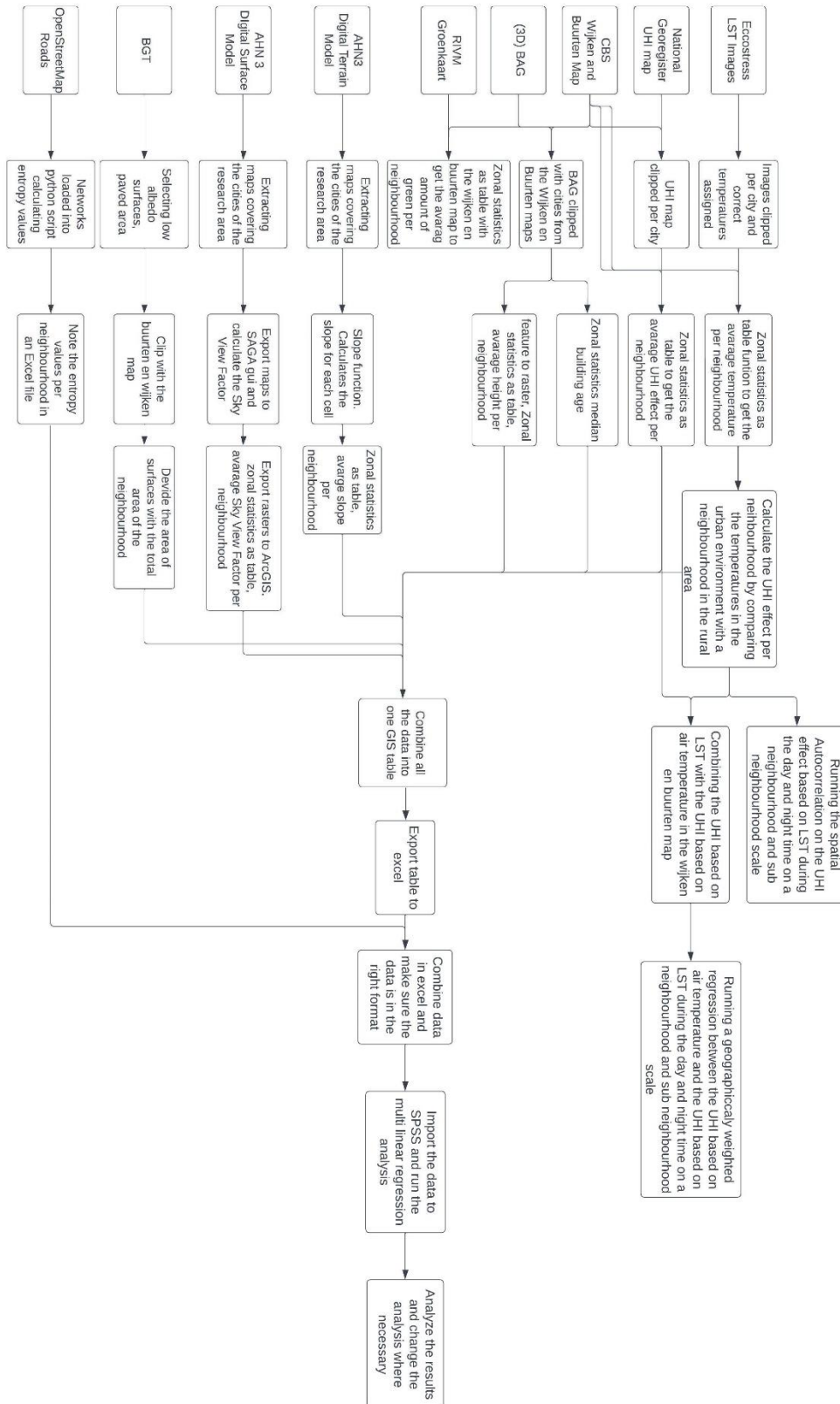
Stone Jr, B., & Rodgers, M. O. (2001). Urban form and thermal efficiency: how the design of cities influences the urban heat island effect. *American Planning Association. Journal of the LST American Planning Association*, 67(2), 186.

- Stone, B., Hess, J. J., & Frumkin, H. (2010). Urban form and extreme heat events: are sprawling cities more vulnerable to climate change than compact cities?. *Environmental health perspectives*, 118(10), 1425-1428.
- Sugawara, H., & Takamura, T. (2014). Surface albedo in cities: case study in Sapporo and Tokyo , Japan. *Boundary-layer meteorology*, 153(3), 539-553.
- Thermal Infrared Sensor (TIRS) | Landsat Science*. (2013, June 19). Landsat Science | a Joint NASA/USGS Earth Observation Program. Retrieved October 19, 2022, from <https://landsat.gsfc.nasa.gov/article/thermal-infrared-sensor-tirs/>
- Tomlinson, C. J., Chapman, L., Thornes, J. E., & Baker, C. J. (2011). Including the urban heat island in spatial heat health risk assessment strategies: a case study for Birmingham, UK. *International journal of health geographics*, 10(1), 1-14.
- Urban heat islands: WUR and urban climate change adaptation*. (n.d.). wur.nl. Retrieved October 12, 2022, from <https://www.wur.nl/en/research-results/research-institutes/environmental-research/show-wenr/urban-heat-islands-wur-and-urban-climate-change-adaptation.htm>
- Urban Heat Island | National Geographic Society*. (n.d.). Retrieved October 12, 2022, from <https://education.nationalgeographic.org/resource/urban-heat-island/>
- Vaidyanathan, A., J. Malilay, P. Schramm, and S. Saha. 2020. Heat-related deaths — United States, 2004–2018. *Morbidity and Mortality Weekly Report* 69(24):729–734.
- Vocht, A. (2019). *Statistische Methoden Syllabus, Faculty of Geosciences* [Print Version]
- Vujovic, S., Haddad, B., Karaky, H., Sebaibi, N., & Boutouil, M. (2021). Urban heat Island: Causes, consequences, and mitigation measures with emphasis on reflective and permeable pavements. *CivilEng*, 2(2), 459-484.
- Weerplaats. (2022a,). *Weer 11 augustus 2022*. Weerplaats. <https://www.weerplaats.nl/weer-11-augustus-2022/>
- Weerplaats. (2022b). *Weer 4 juli 2022*. *Weerplaats*. <https://www.weerplaats.nl/weer-4-juli-2022/>
- Who is at risk to extreme heat*. (n.d.). <https://www.heat.gov/pages/who-is-at-risk-to-extreme-heat>
- Who We Are | U.S. Geological Survey*. (n.d.). <https://www.usgs.gov/about/about-us/who-we-are>
- Wong, K. V., Paddon, A., & Jimenez, A. (2013). Review of world urban heat islands: Many linked to increased mortality. *Journal of Energy Resources Technology*, 135(2).
- Yang, J., Wang, Z. H., & Kaloush, K. E. (2015). Environmental impacts of reflective materials: Is high albedo a 'silver bullet' for mitigating urban heat island?. *Renewable and Sustainable Energy Reviews*, 47, 830-843.
- Zoulia, I., Santamouris, M., & Dimoudi, A. (2009). Monitoring the effect of urban green areas on the heat island in Athens. *Environmental monitoring and assessment*, 156(1), 275-292.

8. Appendix

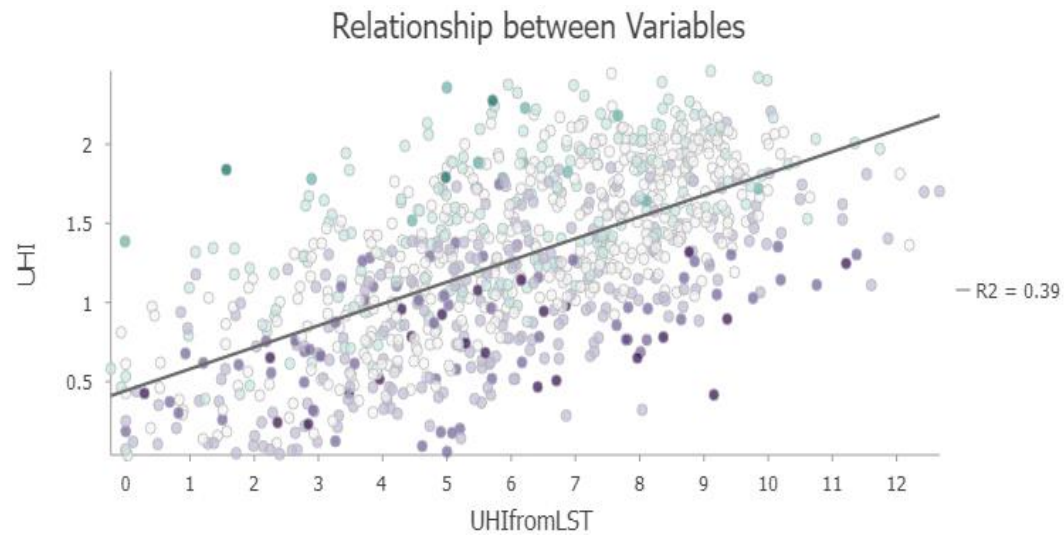
Appendix 1

Flowchart of the methodology



Appendix 2

Regression graph between the UHI based on air temperature and the UHI based on LST on a sub neighbourhood scale during the day.



Appendix 3

Regression graph between the UHI based on air temperature and the UHI based on LST on a sub neighbourhood scale during the night.

